Architecture and dynamics of Precambrian linear megadunes: Galho do Miguel Formation, Mesoproterozoic, South-East Brazil

Áquila Ferreira Mesquita[a*], Giorgio Basilici[a,b], Alexandre Ribeiro Cardoso[a], Carlos Roberto de Souza Filho[a], Nigel P. Mountney[c], Luca Colombera[d], Grace I.E. Cosgrove[c], Juraj Janočko[e], Davi Machado Querubim[a],

[a] Department of Geology and Natural Resources, Institute of Geosciences, University of Campinas, 13083-870, Campinas, São Paulo, Brazil

[b] Centro Regional de Investigaciones Científicas y Transferencia Tecnológica (CRILAR-CONICET), Entre Ríos y Mendoza s/n., 5301, Anillaco, La Rioja, Argentina

[c] Fluvial, Eolian & Shallow-Marine Research Group, School of Earth and Environment, University of Leeds, Leeds LS2 9JY, UK

[d] Dipartimento di Scienze della Terra e dell'Ambiente, Università di Pavia, Via Ferrata 1, 27100, Pavia, Italy

[e] Institute of Geosciences, Faculty BERG, Technical University of Kosice, Letna 9, 040 11, Kosice, Slovakia

*Corresponding author: aquila.fmesquita@gmail.com

ABSTRACT

Recognizing the deposits of linear megadunes in ancient aeolian successions is challenging when the original bedform topography is not preserved. This task is especially difficult in Precambrian aeolian successions due to potential metamorphism and deformation, which obscures primary sedimentary structures. The present study provides a detailed analysis of the depositional architecture of an ~80 m-thick interval of the Mesoproterozoic Galho do Miguel Formation (SE Brazil), for which it has been possible to reconstruct the original morphologies of linear megadunes (or draas) and understand their dynamics. The depositional architecture reveals compound cross-bedded sets, which transition laterally into thick

low-angle cross-stratified sets and planar-parallel sandstone beds. The depositional features indicate the presence of complex megadunes separated by adjoining wide dry inter-megadune areas, which were themselves flooded seasonally by a water table that rose above the depositional surface. Linear megadunes experienced two phases of development: vertical accretion and subsequent episode of lateral migration. During the vertical accretion phase, high sediment supply, typical of Precambrian aeolian systems, and the convergence of winds from two distinct directions promoted high rates of megadune growth, bedform elongation, and the formation of superimposed dunes. The lateral migration phase was characterised by a component of lateral bedform shift relative to the main along-crest sediment transport direction; this prevented preservation of a bimodal pattern of dune cross-strata azimuths. The accumulation of these deposits occurred via a combination of megadune climb that occurred with progressive rise of the water-table level. The water-table rise hindered cannibalization of the lower parts of the migrating megadunes, allowing the accumulation and subsequent preservation of megadune sandstone packages. The rise of the water table was also responsible for the accumulation of thick dry inter-megadune strata. The unusual thickness of linear megadune and inter-megadune deposits of the Galho do Miguel Fomation, as compared with Phanerozoic examples, are attributed to the interplay between the barren conditions of the early Earth, the morphodynamics of the linear megadunes, and the seasonal impact of the water table at the accumulation surface. Without a water-table control, opportunities for megadune accumulation and preservation were likely limited in Precambrian ergs.

Keywords: Erg; Interdune; Wet eolian system; Dry eolian system; Espinhaço supergroup.

1. INTRODUCTION

Linear aeolian dunes and megadunes cover about 40% of the surface area of present-day large sand seas. However, despite their abundance, they are not commonly identified in the ancient geological record (Munyikwa, 2005; Rodríguez-López et al., 2014). During the Precambrian, the absence of

terrestrial vegetation favoured the creation of a bare surface, susceptible to weathering and erosion processes, thus yielding a large volume of sediment for potential aeolian transport and deposition (Eriksson and Simpson, 1998; Eriksson et al., 2005; Bose et al., 2012). Thus, megadunes with high morphological variety were probably more easily constructed in Precambrian aeolian systems than in their Phanerozoic counterparts (cf. Mesquita et al., 2021a; Cosgrove et al., 2023). In contemporary extraterrestrial ergs, where the sedimentary conditions are not dissimilar to those recorded during the Precambrian on Earth, linear-shaped megadunes also dominate the aeolian landscape (Bourke et al., 2010; Radebaugh et al., 2010), suggesting that linear megadune deposits should be common in Precambrian aeolian succession. Yet, few such deposits are recognised in the Precambrian record worldwide (Cosgrove et al., 2021, 2023, 2024). In contrast, preserved Precambrian aeolian deposits rarely exhibit deposits produced by dunes with significant morphological variety; they predominantly comprise of deposits of simple transverse and/or crescentic dunes, and sand sheets (e.g., Tirsgaard and Øxnevad, 1998; Simpson et al., 2002; Catuneanu et al., 2005; Heness et al., 2014; Bállico et al., 2017; Basilici et al., 2020; Cosgrove et al., 2023).

The apparent lack of linear megadune systems in Precambrian continental settings might be associated with two main factors. First, it is possible that megadune systems may have been constructed over Proterozoic landmasses, but the absence of sand-fixing agents (e.g., water, soil, or vegetation) made the sand susceptible to re-working, thereby preventing long-term aeolian accumulation and preservation (cf. Eriksson and Simpson, 1998; Eriksson et al., 2005; Basilici et al., 2021; Mesquita et al., 2021a). Consequently, only the lowermost portions of megadunes may be preferentially preserved (e.g., Deynoux et al., 1989; Jackson et al., 1990; Tirsgaard and Øxnevad, 1998; Heness et al., 2014), for example via bedform climb or gradual water-table rise. Second, modern linear mega-bedforms are abundant in aeolian environments where the sand availability is not especially high (Tsoar, 1989; Mountney, 2006b). In Precambrian ergs, their development could have been hampered or somehow restricted by the higher rates of sand supply and availability at that time, such that other bedform types developed preferentially. Therefore, factors that apparently limited the construction of linear megadunes and prevented their

77 complete preservation could be the main reasons why few such examples of these bedform types are
78 identified in Precambrian aeolian successions.

79 The identification of the deposits of linear megadunes is most readily accomplished when
80 exceptional mechanisms preserve all (or the great majority) of the original dune morphology. Such cases
81 most obviously arise in response to (i) covering of the bedforms by lava flows (e.g., Clemmensen, 1988;
82 Scherer, 2002), or (ii) passive flooding of the bedforms due to marine transgression (e.g., Rodríguez-
83 López et al., 2012; Scotti and Veiga, 2019; Shozaki and Hasegawa, 2022). Yet the reconstruction of
84 ancient linear megadunes presents many additional difficulties: (i) the deposits of linear megadunes tend
85 to have an internal architecture similar to that of the deposits of crescentic dunes (Rubin and Hunter,
86 1985); and (ii) linear bedforms tend to develop over large deflation surfaces, where the potential for their
87 long-term aeolian accumulation and preservation is very limited (Mainguet and Chemin, 1983).

88 To date, only limited research has addressed the study of the depositional architecture of linear
89 megadunes in the ancient sedimentary record (e.g., Chrintz and Clemmensen, 1993; Scherer, 2000;
90 Besley et al., 2018; Scotti and Veiga, 2019), and identification of such dune types from Precambrian
91 successions is rare (Cosgrove et al., 2023). This reflects the complexity of recognising their deposits in
92 cases where the original dune topography is not preserved. As a result, there are relatively few examples
93 where aeolian successions can be demonstrably shown to be the deposits of linear megadunes. This
94 hinders the recognition of the depositional architecture and morphodynamic behaviours of mega-
95 bedforms in Precambrian erg successions. Moreover, the following can be hypothesised: (i) the
96 morphodynamics of linear megadunes were distinct in Precambrian ergs due to the unique sedimentation
97 pattens that were in operation during that time; and that, therefore, (ii) these bedforms produced a
98 distinctive depositional architecture that differs from deposits in Phanerozoic successions.

99 To investigate this hypothesis, the present study has analysed the Mesoproterozoic aeolian
100 succession of the Galho do Miguel Formation. This quartz arenite succession is located in Serra do
101 Espinhaço (Minas Gerais, SE Brazil). It is revealed by excellent lateral and vertical exposures (Fig. 1)
102 (Mesquita et al., 2021a). The progressive rise of the water-table level, concomitant with the construction

of the megadunes, allowed their accumulation and contributed to preservation (Abrantes Jr et al., 2020; Basilici et al., 2021). Through the description of the internal architecture and the interpretation of the linear megadunes this paper has three objectives: (i) to provide sedimentological and stratigraphic observations for identifying linear megadunes in ancient aeolian records; (ii) to discuss the dynamic controls that governed the construction and accumulation of Precambrian linear megadunes; and (iii) to compare Precambrian linear megadune deposits with Post-Silurian examples to discern the effect of a vegetated Earth on these megabedforms.

2. LINEAR MEGADUNES OVERVIEW

Linear mega-bedforms have crestlines elongated parallel to the net sand-transport direction (Hesp et al., 1989). These megadunes exhibit significant length, often exceeding 20 km, with elongated ridges, an asymmetric cross-sections profile, and a peaked crest orientated <15° from the resultant sand drift direction. By contrast, transverse dunes have crestlines oriented at an angle >75° with respect to the resultant sand drift direction (cf. Hunter et al., 1983). Linear megadunes maintain a regular spacing, migrate in a parallel to similar neighbouring bedforms, and exhibit a low ratio of megadune to inter-megadune areas (Lancaster, 1982, Bristow et al., 2000).

Linear megadunes develop in bimodal or multidirectional wind regimes. Each wind tends to interact with the dune at an oblique angle ranging from 30° to 40°, causing the airflow on the lee side to deflect almost parallel to the crestline (Lancaster, 1982; Rubin et al., 2008). The dune lee slope may alternate sides locally along the bedform crestline. The patterns of erosion and deposition, as well as the migration rates of these megadunes, depend on the incidence angle between the winds and the crest line (Tsoar, 1983; Tsoar, 2001). When this incidence angle is less than 40°, the velocity and the angle of the wind deflection tend to be high, encouraging a high longitudinal sand transport and dune elongation (Tsoar, 1989; Lucas et al., 2015) (Fig. 2A). Conversely, angles exceeding 40° result in reduced net wind velocity and preferential deposition on the lee flanks (Tseo, 1993, Tsoar, 1989). Additionally, changes in the velocity, direction, and frequency of the incident airflows may occur due to fluctuation of wind-pattern

129 circulation in different seasons; this results in asymmetric transport of sand across the crest, shaping them
130 into sinuous-crested, meandering forms (Tsoar, 2001) (Fig. 2B).

131 Linear megadunes may experience lateral displacement in addition to longitudinal movement
132 (Rubin and Hunter, 1987; Tsoar et al., 2004). In the case of an asymmetrical wind regime (i.e., where one
133 wind direction in a bimodal regime has a greater potential sand-carrying capacity), one of the dune flanks
134 tends to undergo a higher rate of sand deposition (Rubin et al., 2008, Bristow et al., 2005). In such cases,
135 the main sand drift direction is not strictly parallel to the dune crestline. This induces a long-term net lateral
136 movement (crabbing) of linear dunes (Tsoar et al, 2004, Bristow et al., 2005, Rubin et al., 2008, Bristow
137 et al., 2007) (Fig. 2A, B). This movement is very slow and occurs simultaneously with along-crest dune
138 elongation (Hesp, 1989; Davis et al., 2020). An asymmetric bimodal wind regime prevails in most ergs,
139 such that lateral migration is expected in most linear dune systems (Wilson, 1973, Tsoar et al., 2004; Pye
140 and Tsoar, 2009).

141 The scarcity of documented linear megadune deposits in the ancient geological records – and
142 especially in the Precambrian record – despite their abundance in present-day ergs, has been attributed
143 to a failure to recognise the preserved internal sedimentary architecture of such bedforms because the
144 component of lateral migration preferentially preserves deposits that superficially appear similar to those
145 of transverse dunes (Tsoar et al., 2004). Studies by Rubin and Hunter (1985) and Rubin (1987)
146 demonstrate that linear dunes can move sideways, through net deposition on one flank and net erosion
147 on the other, similarly to transverse migrating dunes. Thus, only one flank of the dune is typically
148 preserved, leading to the loss of evidence of the original bimodal pattern of foreset dip-azimuths (Rubin
149 and Hunter, 1985, Scotti and Veiga, 2019). Figure 1 shows a schematic model to indicate how the
150 accumulation and preservation of linear dunes deposits is expressed in symmetric and asymmetric wind
151 regimes.

152 Linear bedforms can be classified based on their morphological characteristics or
153 morphodynamics. The morphological classification regards the number of lee faces that they possess
154 (McKee, 1979; Tsoar, 2001), whereas the morphodynamic classification considers the alignment of their

crestlines in relation to the main sand drift direction. Thus, they can be classified as linear (or seif) dunes or longitudinal dunes, respectively. Following the morphological classification of McKee (1979) and Wilson (1972), three types of linear dunes can be distinguished, ordered by increasing size and complexity: simple, compound, and complex. Simple dunes consist of a single migrating dune, whereas compound and complex dunes represent large-scale parent bedforms which themselves support superimposed child bedforms of a similar or different morphological form, respectively (Mckee, 1979, Pye and Tsoar, 2009).

In a general sense, compound linear megadunes are arranged by superimposed dunes with similar morphology, which migrate over the leeside of a larger linear bedform, while complex linear megadunes are composed of superimposed dunes of different size and morphologies migrating obliquely to lee sides of the main linear bedform (Wilson, 1973; Pye and Tsoar, 2009) (Figs. 2A, B).

3. GEOLOGICAL SETTING

The Galho do Miguel Formation is a unit c. 1500 m thick of the Espinhaço Supergroup, deposited in a complex and polycyclic rift basin developed over the São Francisco Craton during the Paleoproterozoic to Mesoproterozoic (Almeida-Abreu, 1995; Martins-Neto, 2000). The Espinhaço Supergroup encompasses a metasedimentary sequence spanning 1200 km in a north-south direction in southeastern Brazil. The deposits under investigation are situated within the Southern Espinhaço Domain, where the sedimentary succession was partially deformed and metamorphosed to a low-grade greenschist facies during the Brasiliano Orogenic Cycle (ca. 650–500 Ma) (Brito Neves et al., 2014). The Lower Espinhaço Sequence is dated to the Statherian period and comprises fluvial and aeolian deposits of the Bandeirinha Formation and alluvial-fan deposits of the São João da Chapada Formation (Chemale Jr et al., 2012; Santos et al., 2013; Simplício and Basilici, 2015). By constrast, the Upper Espinhaço Sequence is composed of the Sopa-Brumadinho Formation, Galho do Miguel Formation and the Conselheiro Mata Group, deposited during the Stenian period in fluvio-lacustrine, aeolian and shallow-marine environments, respectively (Chemale Jr et al., 2012; Santos et al., 2013, Santos et al., 2015).

The Galho do Miguel Formation comprises a succession of aeolian metaquartz arenites commonly exposed in the southern portion of the Espinhaço Range (c. 5000 km²) (Martins-Neto, 2000; Chemale Jr et al., 2012; Santos et al., 2015). This formation shows small- to large-scale cross-stratified sets (0.1 to 8 m thick) and planar-parallel strata (0.1 to 6.5 m thick) deposited by aeolian dunes/megadunes, interdunes and sand sheets. Despite the low-grade metamorphism, the depositional architecture and the original sediment texture of these deposits are well-preserved (Dussin and Dussin, 1995; Martins-Neto, 2000; Mesquita et al., 2021a). Recent studies have demonstrated that the Galho do Miguel Formation represents a typical record of a hybrid aeolian system originated by coeval deposition of dry and wet sub-environments (Abrantes Jr et al., 2020; Basilici et al., 2021). Preserved deposits associated with wet aeolian sub-environments are concentrated in the northern sector of the unit and record the predominant deposition of simple dunes, wet interdunes, sand sheets, and salt flats. Conversely, deposits linked to dry aeolian subenvironments are concentrated in the southern sector of the formation and originate from widespread dry interdune and dune/megadune activity (Basilici et al., 2021; Mesquita et al., 2021b). The analysis of dip-azimuth foreset measurements indicates that the trend of palaeodune migration (simple and compound/complex dunes) predominantly occurred towards NE in both settings (Abrantes Jr et al., 2020; Mesquita et al., 2021a; Basilici et al., 2021). Geochronological studies suggest Stenian age (1.2-1.0 Ga) as the maximum age of sedimentation for the Galho do Miguel Formation (Chemale Jr et al., 2012; Santos et al., 2015).

4. METHODS

Depositional architecture and facies analysis were performed on exposures located at two primary sites within the south-central portion of the Galho do Miguel Formation: Serra do Pasmar and Morro Batatal. In these areas the depositional architecture of megadune deposits can be observed in vertically and laterally extensive exposures, reaching heights of up to 30 metres and extending over 100 metres. Complementary data of sedimentary facies and depositional architecture were also collected from

exposures along a 35 km-long cross-section, extending from Barão de Guacuí city to Sempre Vivas National Park.

The recognition of architectural elements has been based on (i) sedimentary structures, (ii) orientation and distribution of the forest dip azimuths, (iii) thicknesses of cross-stratified sets and variations in their geometry, and (iv) the hierarchy of the bounding surfaces. Four sedimentary graphic logs (with a cumulative total length of 256 m), photomosaics and 2D interpretative architectural panels portray the lateral distribution, geometry and stratigraphic relationships between the architectural elements and bounding surfaces. The type and hierarchy of the bounding surfaces are defined according to identification criteria defined by Brookfield (1977) and are interpreted following the methods of Kocurek (1981, 1988, 1991, 1996). The net orientations of megadune migration were determined from dip-direction data of the planes of cross-strata and their relationship with superimposed bounding surfaces, following the stereonet reconstruction technique proposed by Rubin and Hunter (1983), Havholm and Kocurek (1988) and Chrintz and Clemmensen (1989). All data collected from forest dip-azimuth and bounding surfaces were plotted on stereonets and rose diagrams after applying correction techniques to remove the effects of tectonic tilting. The attitude of planar-parallel strata that contain marks of aqueous vortex ripples was used as a datum and to define a palaeohorizontal surface. Despite the low-grade metamorphism experienced by these rocks, this study adopts a sedimentological nomenclature to describe the studied succession due to the preservation of the original sedimentary features.

This study employs the morphological classification and dune hierarchy proposed by McKee (1979) and Tsoar (2001). Notwithstanding, large bedforms can be named in a variety of ways: compound dunes (McKee, 1979), draas (Wilson, 1973), megadunes (Pye and Tsoar, 2009). In this work, the terminology "megadune" is used to refer to a set of superimposed dunes migrating over a larger bedform, as proposed by Pye and Tsoar (2009).

5. DEPOSITIONAL ARCHITECTURE

The deposits are characterised by well-sorted and very fine- to coarse-grained quartzarenite, generally made of monocrystalline quartz grains (c. 90%). The Galho do Miguel Formation comprises an alternation between cosets of cross-stratified sets and wavy and planar-parallel bed sandstones. The latter units are interpreted as sand sheet deposits (Mesquita et al., 2021a). The following description focuses only on the stratigraphic interval originated by megadune/dune and interdune deposition (Fig. 3). Three types of architectural elements were recognised: (i) compound cross-bedded and low-angle cross-bedded sets; (ii) simple cross-bedded sets; (iii) planar-parallel sandstone strata (Table 1). All these elements occur in a similar frequency in the two studied sites, and the following description is ordered according to morphological and sedimentary criteria: dune deposits (compound and simple) and interdune strata.

4.1. Compound cross-bedded and low-angle cross-bedded sets (megadune element)

5.1.1. Description

This architectural-element type is characterized by the interfingering of two main lithofacies: (i) compound cross-bedded sets, and (ii) low-angle cross-bedded sets (Fig. 3). The first lithofacies comprises individual sets of trough cross-stratification that are 2 to 8 m thick and 7 to 10 m wide in palaeotransport-transverse sections. They are organised in a compound arrangement, in which the foresets show an asymmetrical profile (Figs. 4, 5). In parallel and oblique sections to the palaeotransport, these deposits are expressed as compound wedge-shaped sets (sometimes lens- or tabular-shaped beds) of cross-stratifications, 2 to 6 m thick and 8 to 15 m wide (Fig. 6). The dimensions and geometries of the individual sets of compound cross-bedding are variable throughout the entire succession, being 1.3 to 5.5 m in thickness and 2 to 10 m in width. The sets are commonly bounded by second-order bounding surfaces, described below (Figs. 5, 6). The cross-stratification is mostly tangential to the underlying bounding surface and is inclined between 15° and 31° (Fig. 4). Locally, in palaeotransport-parallel sections, the

lowermost part of foresets shows interdigitations of wedge-shaped lamina sets of different thicknesses and grain sizes, recognised as wedges of grainflow and subcritical climbing translatent strata (Fig. 7A) (*sensu* Hunter, 1977). The grainflow strata are dominant (c. 80% of the foresets composition) and appear as fine- to medium-grained sandstones that are 15 to 40 mm thick and massive, whereas the subcritical climbing translatent strata comprise fine- to coarse-grained sandstones that are 5 to 10 mm thick and arranged in inversely graded laminae (c. 20% of the cross-stratification composition). Cross-stratified toe-set deposits mostly display an encroached or abrupt contact with underlying planar-parallel sandstone strata in palaeotransport-parallel sections (Figs.5, 7B).

The azimuthal dip of the foresets exhibit a wide distribution between 010° and 190°. Locally, it is possible to recognise a bimodal distribution of the foreset dip-azimuths with two main ranges: NE-SE and NW-SW (Fig. 4D), but, in general, they align towards NE. In the Morro do Batatal locality, the mean value of the forest dip-azimuths is towards c. 060° (Fig. 5D), whereas in the Serra do Pasmar locality, the mean value is towards c. 080° (Fig 6D).

The "low-angle cross-bedded sets" constitute discontinued tabular- or lens-shaped sets of low-angle cross-stratification, 2 to 5.5 m thick and 3 to 10 m wide, that are often laterally connected to the lowermost part of foresets of the compound cross-bedded sets deposits (Figs 5, 6). The lateral connectivity between them occurs as a progressive downwind transition of the foresets dip-angle, from high-angle (>15°) to low-angle cross-stratification in sections parallel or oblique to the palaeotransport (Fig. 7C, 7D). Overall, this transition is followed by the progressive dominance of planar-parallel sandstone (dry interdune deposits) strata downwind in gradational contact (Figs.6, 7D). Abrupt contacts between "compound cross-bedded sets" and overlapped "low-angle cross-bedded sets" are common (Figs. 5, 6). The average foreset-dip azimuths are towards 120° and the foresets exhibit a high-spread dip-direction distribution, mainly between 40° to 190° azimuth (Fig.8A). Despite the lateral relationship of these deposits with "compound cross-bedded sets", they show a general tendency of clockwise oblique palaeotransport to each other (c. 40°). The abrupt contact between these lithofacies units is common (Figs 5, 6). In a few places, discontinuous beds, 10 to 20 mm thick and up to 1 m wide, containing small

vortex ripple marks are present in the lowermost part of low-angle cross-stratifications. The vortex ripples are characterised by slightly asymmetric profile, straight or slightly sinuous crestlines and exhibit peaked or rounded crests with local bifurcations (Fig. 8D). The ripple index and ripple symmetry index of these structures are 10.2 and 1.2, respectively.

Three orders of bounding surfaces commonly delimit the architectural element. The first-order surface represents a flat and low-angle inclined bounding surface (< 10°) laterally continuous for 10 to 50 m along transverse and oblique sections relative to the palaeotransport trend (Figs. 5, 6). First-order bounding surfaces may display an irregular or undulated form, whereby they exhibit small depressions and steps (Fig. 8C, 8D). These surfaces may delimit the top and the bottom of lithofacies that constitute this architectural-element type.

Second-order bounding surfaces limit the individual sets of cross-strata. This type of surface is recognised by the concave-up and inclined geometry with variable dip angles (05° to 18°) and extents of up to 15 m and 10 m in sections oblique and parallel to the palaeotransport, respectively (Figs. 4, 6). Locally, in sections perpendicular to the palaeotransport, it was possible to identify a bidirectional trend of the dip azimuths of these surfaces. This characteristic is recognised by the presence of two main clusters of poles opposites to each other (Fig. 4E). Overall, this type of surface demonstrates a unimodal and narrow distribution in dip azimuths, displaying a dip azimuth towards 115° and 146° in the deposits of the Morro do Batatal and Serra do Pasmar localities, respectively (Fig.5E, 6E).

Third-order bounding surfaces occur inside the individual sets and crosscut pre-existing foresets in parallel and oblique palaeotransport sections. They are abundant and occur in a random distribution, limiting packages of foresets strata that are arranged oblique to each other, with orientations of foresets in adjoining stratal packages varying by up to 12° (Fig. 6C).

5.1.2. Interpretation

The sandstone bodies composed of well-sorted grains and arranged in cross-stratified sets, with tangential or trough cross-stratifications, indicate deposits originated by the migration of aeolian dunes

(Kocurek, 1991; Mountney, 2006a, Basilici et al., 2021). The predominance of grain-flow strata in the lowermost part of the tangential cross-stratifications and their wide thickness range indicates: (i) well-developed dune slipfaces (Hunter, 1977) and (ii) dunes of varying height (from 2 to 30 m according to the empirical relationship proposed by Kocurek and Dott, 1981, and Romain and Mountney, 2014).

The frequent occurrence of intermittent and erosional bounding surfaces cross-cutting and delimiting the foresets define the compound arrangement of the cross-stratified beds (Rubin and Hunter, 1983; Rubin and Carter, 2004). This architectural organisation suggests that the sand accumulated by the development of superimposed smaller dunes over a large aeolian bedform (megadune) (Brookfield, 1977; Kocurek, 1981; Rubin and Hunter, 1983). The “first type” of bounding surface that delimits the packages of compound cross-bedded sets represents the first-order surface type A of Basilici et al. (2021). This surface type represents an inter-megadune surface, which is originated by mega-bedform migration over inter-bedform areas (Kocurek, 1981; Kocurek, 1988; Clemmensen, 1989). The undulated- or irregular-shaped interdune erosional surface suggests seasonal shifts in the inter-megadune reworking rates during bedform advance (Mountney, 2012). Two potential causes can explain those seasonal fluctuations. First, the development of wet/damp accumulation surfaces may hamper the sand removal from interdune areas by turbulent airflows in front of the dune lee face during its migration (e.g., Mesquita et al., 2021a; Basilici et al., 2021). This condition probably led to development of irregular and undulate interdune surfaces, locally characterised by small depressions and step-like geometries (cf. Kocurek, 1981; Kocurek and Day, 2018). Second, seasonal shifts in wind-sand saturation and/or in its potential sand-transport capacity, potentially caused by the development of wet/damp deflationary surfaces, which determined changes in bedform migration rates and angle of climb. In turn, this process could have produced irregular erosion of the adjoining interdune flats by dune advance, now expressed as irregular-shaped first-order bounding surfaces (Mountney, 2006b; Mountney, 2012). In general, both conditions may have been driven by the near-surface water table over the accumulation surface, which provided a reduction of the sand availability to wind transport and, consequently the speed of bedform migration, and the decreased potential of sand removal from interdune flats by dune advance (cf. Mountney and

Thompson, 2002; Mountney and Jagger, 2004). The presence of small vortex ripples close to the base of the dune lee face supports the hypothesis of variations in the water-table level relative to the dry accumulation surface (e.g., Mountney and Jagger, 2004; Basilici et al., 2020). Bounding surfaces of the second type correspond to the second-order bounding surfaces of Brookfield (1997); they are interpreted as superimposition surfaces (Brookfield, 1977; Rubin and Hunter, 1983). The presence and distribution of these surfaces, which produce a compound arrangement of cross-bedded sets, presuppose the development of smaller dunes that migrated obliquely and over the lee slope of a larger bedform, as a megadune (Rubin, 1987; Rubin and Hunter, 1983, Pye and Tsoar, 2009). Bounding surfaces of the third type are equivalent to the third-order bounding surfaces of Brookfield (1977), which are interpreted as reactivation surfaces (Kocurek, 1981). Reactivation surfaces are generally associated with shifts of primary airflow direction or speed, producing a partial erosion of dune lee slopes (Kocurek, 1991, Kocurek, 1996). However, the abundance of these surfaces might also signify a genetic link with dunes with sinuous crestlines; meandering shifts of the dune crestline during bedform migration can produce partial erosion of the avalanching faces and, consequently, the formation of inclined truncating surfaces within accumulated cross-bedded sets (Lancaster, 1982; Scherer, 2000; Mountney and Howell, 2000; Rubin and Carter, 2004).

The lateral connection between the low-angle cross-bedded sets and the compound cross-bedded sets suggests deposits produced from sedimentation in plinth areas surrounding mega-bedforms (Pulvertaft, 1985; Havhlom and Kocurek, 1988). Evidence that supports this interpretation includes: (i) the progressive downwind change in the foreset dip-angle, with an asymptotic and gradual transition to interdune wind-ripple laminations, and (ii) a similar trend in sand palaeotransport between the low-angle cross-strata and the foreset dip-azimuths of megadune strata (Pulvertaft, 1985; Clemmensen, 1989; Scherer, 2000; Mountney, 2006b). The high spread azimuths of dune cross-strata representative of dune plinth deposits suggest a markedly curved megadune crestline, as commonly observed in modern megadune systems (cf. Lancaster, 1982; Livingstone, 1989). The presence of small vortex ripples

randomly distributed in these strata suggest the seasonal presence of stagnant water close to the lee face plinth during megadune advance (Pulvertaft, 1985; Mountney, 2006b).

The depositional architecture of these sandstone bodies, mainly featuring compound sets of cross-strata bounded by superimposition surfaces, suggests that they are preserved deposits of megadunes with markedly curved crestlines. The variable thickness of the superimposed sets may reflect the migration and climbing of superimposed dunes of different sizes and angles of climb (Mountney and Howell, 2000; Dias and Scherer, 2008, Mountney, 2012). These characteristics are associated with the large variety of geometries and thickness of the compound cross-bedded sets. They can be related to the development of dunes of variable morphologies and sizes superimposing mega-bedform slipfaces (Rubin and Hunter, 1982; Mesquita et al., 2021a); these may encompass, for example, transverse dunes and oblique dunes migrating coevally (e.g., Havholm and Kocurek, 1988; Clemmensen and Blakey, 1989; Dong et al., 2004). According to the classification of McKee (1979) and Tsoar (2001), this architectural-element type is interpreted as a complex megadune.

5.2. Simple cross-bedded sets (simple dune element)

5.2.1. Description

The "simple cross-bedded sets" element is interbedded with the "compound cross-bedded sets and low-angle cross-bedded sets" element. It comprises around 15% of the cumulative thickness of the measured succession. This element-type consists of simple sets of tangential cross-stratifications with tabular-shaped geometry, up to 2 m thick and 4 to 40 m wide in palaeotransport-parallel cross-sections (Figs. 4, 9A). Locally, wedge-shaped laminations of different thickness and grain sizes, recognised as grainflow and subcritical climbing translatent strata (*sensu* Hunter, 1977), occur interdigitated in the lowermost parts of cross-stratified sets (Fig. 9B). Grainflow strata are the predominant cross-stratification type and comprise massive depsoits of fine- to medium-grained sand grains 20 to 55 mm thick. Subcritical climbing translatent strata appear as fine- to coarse-grained deposits, 4 to 15 mm thick, arranged in an

apparent coarsening upward trend inside individual laminae. Individual laminae can extend for up to 80 mm along the foresets. The foreset dip azimuths show an unimodal pattern and low-spread distribution (045° to 120°), with mean values of the azimuths towards 080° and dip angles between 22° to 30° (Fig. 9C).

The individual cross-stratified sets are delimited by two types of bounding surfaces, whose identification is based on their geometry and lateral extent (Figs. 4C, 9A). The first type of surface represents a flat, irregular, and near-horizontal bounding surface (< 10°), 30 to 60 m wide, in palaeotransport-parallel sections (Figs. 4C, 9A). These surfaces bound the top and the bottom of simple cross-bedded sets. The second type of bounding surface occurs within the set and, in palaeotransport-parallel sections, represent erosional concave upward surfaces that truncate the foresets at angles of 10° to 15° in the lowermost parts of sets (Figs. 4C, 9A). They are often crosscut by the first bounding surface type at their top and bottom. This surface type also delimits the foresets with dip-azimuths oblique to each other (between 5° to 15° of obliquity). The "simple cross-bedded sets" element tends to occur at the base of the studied sedimentary succession and is generally overlain by deposits of "compound cross-bedded and low-angle cross-bedded sets" (Fig. 3).

5.2.2. Interpretation

Well-sorted sandstone beds arranged in simple sets of tangential cross-stratifications suggest an origin by construction and migration of simple aeolian dunes (Hunter, 1977; Kocurek, 1991). This hypothesis is also supported by the interdigitation of wedges of grainflow and subcritical climbing translatent strata in the lowermost part of cross-strata, which are due to the alternation of sand avalanches and the climbing of wind ripples over the dune slipfaces during the dune advance, respectively (Sharp, 1963; Hunter, 1977; Mountney, 2006). The thickness and predominance of grainflow strata also reveal that the simple dunes (i) possessed well-developed slipfaces, (ii) undertook high rates of migration, and (iii) had heights in excess of 15 m (cf. Kocurek and Dott, 1981). Additionally, the planar-shaped sets of cross-strata imply continuous rates of dune migration and a climb angle that did not vary over time, thereby resulting uniform partial erosion of interdune areas in response to ongoing dune migration over interdune

surfaces (Mountney and Howell, 2000; Mountney, 2012; Mesquita et al., 2021). This process was probably due to high sediment supply and uninterrupted and constant sand availability, which maintained a sand-supersaturated airflow and caused high rates of dune migration (Loope and Simpson, 1992, Mountney and Jagger, 2004, Mountney, 2012). Inferences of well-developed dune slipfaces and palaeodune height also corroborate this palaeoenvironmental condition. In contrast, the absence of interstratified interdune deposits and the limited thickness of the individual cross-bedding sets suggests a low-angle of dune climb, as is common for transverse dune systems (Mountney and Howell, 2000; Dias and Scherer, 2008). Therefore, the simple cross-bedded sets element is interpreted as the preserved product of simple transverse or crescentic dunes, which migrated towards NE, as demonstrated by the trend and unimodal distriubution of foreset azimuths with low spread (Rubin, 1987; Kocurek, 1991, Scherer, 2000, Mountney, 2006a).

The first type of bounding surface coincides with the first-order bounding surface of Brookfield (1977), and is interpreted as an interdune surface. This surface results from the near-complete erosion of interdune areas as consequence of low angle of climb during the migration of aeolian dunes (Kocurek, 1981; Kocurek 1988). The absence of sedimentary features indicative of a wet surface associated with this element type suggests that aeolian construction and accumulation occurred in a dry environment (Mountney 2006b, Mountney, 2012). Thus, the absence of sand-accumulating agents (e.g., water or vegetation) left the sediments accumulated in the interdune areas susceptible to later removal by advancing dunes, producing large interdune erosion surfaces that delimit the individual dune cross-bedding sets (Kocurek, 1981a; Rubin, 1981a; Mountney and Jagger, 2004; Hême de Lacotte and Mountney, 2022). The second type of bounding surface corresponds to the third-order bounding surface of Brookfield (1977). This surface is identified as a reactivation surface (Kocurek, 1991, Kocurek, 1996).

5.3. Planar-parallel sandstone strata (Dry inter-megadune element)

5.3.1. Description

The "planar-parallel sandstone strata" consist of laminated sandstones organised in tabular- or lens-shaped beds. The tabular-shaped beds are 4 to 6 m thick and 10 to 100 m wide, whereas the lens-shaped beds are 0.5 to 4 m thick and up to 10 m wide along of the measured exposures (Figs. 6, 10A, 10B). However, most of the strata comprise a tabular-like geometry over tens of metres in palaeowind-parallel or oblique sections and exhibit a regular spacing with the interstratified megadune cross-strata throughout the studied succession (Figs. 5, 6). They are composed of horizontal to sub-horizontal laminae (< 5° inclined), 5 to 10 mm thick, each of which shows an apparent upward inverse grading (Fig.10C). Thin strata of ripple cross-laminations, 5 to 10 mm thick, correspond to less than 5% of the total thickness of this architectural element type (Fig. 10D). In vertical section, the cross laminations are asymmetric and rounded or peaked crests are evident (Fig. 10D). On the bedding surface, the ripple marks display a straight to sinuous crestline with some bifurcations and regular spacing of 8 mm (Fig. 8B). The ripple index and ripple symmetry index are 2.4 and 1.3, respectively.

“Planar-parallel sandstone strata” are usually interstratified with the “compound cross-bedded and low-angle cross-bedded sets” element (Figs. 4, 5, 6). Three types of stratigraphic relationship between them are seen, which are described according to their exposure frequencies: (i) gradational, (ii) encroached and (iii) abrupt. The gradational contact is recognised in parallel sections to the foreset dips and represents the lateral and progressive downwind transition of dip-angle from high- to low-angle cross-strata (Figs. 6, 9). Downwind, the transition is followed by the continued dominance of plinth deposits over planar-parallel sandstone strata (Figs. 5, 7D). This type of contact is the most common with dune cross-bedding sets and represents c. 60% of identified contacts. The encroached contact consists of an intertonguing relationship between foresets toes with underlying planar-parallel sandstone strata (Figs. 4,6, 7D). This contact represents an alternation of wedges of grainflow and subcritical climbing translatent strata in the lowermost portions of foresets. The abrupt contact is represented by a sharp surface between the foresets of “compound cross-bedded sets” lithofacies and "planar parallel sandstone strata" elements. It occurs, in sections parallel to the sediment-palaeotransport, as an extensive, near-horizontal, flat, or

457 undulating surface, recognised and described in the previous sections as the first-order bounding surface
458 of Brookfield (1977) (Figs. 5, 10).

459 *5.3.2. Interpretation*

460 The horizontal to sub-horizontal laminated sandstone beds that show inversely graded laminae are
461 attributed to subcritical climbing translatent strata, which were formed by the migration and climbing of
462 wind ripples over flat surfaces of aeolian deflation (Sharp, 1963, Hunter, 1977). The ripple marked upper
463 bedding surfaces record deposition in subaqueous conditions due to wind-induced oscillatory flows in
464 flooded areas (Basilici et al., 2021; Mesquita et al., 2021a). The asymmetrical profiles of the ripple strata,
465 the rounded or peaked crests, and the straight to sinuous crestlines, suggest development from oscillatory
466 and combined flows. Moreover, the regular ripple spacing demonstrates a constant wave period on the
467 water surface (Bagnold, 1946; Collinson and Mountney, 2019). Based on ripple description, the estimated
468 water depth responsible for the generation of these ripple marks were up to 0.25 m, according to the
469 empirical methods of Immenhauser (2009) (see the Supplementary Material of Basilici et al., 2020). The
470 development of small and shallow ponds was possibly associated with oscillations of the near-surface
471 water table (Mesquita et al., (2021a; Basilici et al., 2021). Despite the presence of wet/damp features, this
472 architectural element accumulated in generally dry conditions.

473 The interstratified arrangement of this element type with superimposed dune cross-sets, together
474 with their sedimentological features, suggests deposits created in dry inter-megadune flats (or interdraas)
475 surrounding mega-scale bedforms (Dong et al., 2004; Abrantes Jr., 2020; Wadhawan, 2020). The lens-
476 shaped bed geometry and the variable thickness of these deposits propose seasonal changes in the dune
477 migration rate and/or climb angle of the dunes through time, producing non-uniform interdune
478 cannibalisation and concave-up (or irregular) bounding surfaces (Loope and Simpson, 1992; Dias and
479 Scherer, 2008; Mountney, 2012; Mesquita et al., 2021b -their Fig. 7). In contrast, the tabular-shaped bed
480 geometry suggests a uniform accumulation and erosion of interdune deposits during the passage of
481 migrating dunes. This feature also indicates a stable angle of climb during bedform migration, producing
482 a long-term accumulation of inter-megadune strata, albeit with accumulated deposits of limited thickness

(cf. Loope and Simpson, 1992; Mountney, 2012; Mesquita et al., 2021b - their Fig. 7). The characteristic interbedding of these beds with compound cross-strata suggests the original presence of large and open inter-megadune corridors, which may have been regularly spaced (Dong et al., 2004; Abrantes Jr., 2020; Mesquita et al., 2021b). Additionally, the geometry and thickness of interdune strata may also imply phases of periodical expansion and contraction of inter-bedform corridors (Jones et al., 2016). In this context, the maximum extent of interdune areas and their maximum sand accumulation rate occurred during periods of limited dune migration (Mountney and Thompson, 2002; Mountney, 2006b; Mountney, 2012).

The stratigraphic relationship between dune and interdune deposits reveals three different morphodynamic patterns of cannibalisation and accumulation of sand inter-megadune flats in studied deposits. The encroached and gradational contacts imply the coexistence and coeval accumulation of aeolian dunes and adjoining dry inter-megadunes over time, suggesting a synchronous migration of dunes and interdunes in the main sand-drift direction (Pulvertaft, 1985; Mountney and Thompson, 2002; Mountney, 2006b). In general, the encroached and gradational contacts require low rates of interdune cannibalisation during dune migration, allowing the partial erosion of inter-megadune deposits and their long-term accumulation through burial by the succeeding migrating dunes (Pulvertaft, 1985; Mesquita et al., 2021b). Encroached contacts represent seasonal changes in the dune slipface angle over interdune areas, producing variation of interdune reworking of the advancing dune (Pulvertaft, 1985; Mountney, 2006b; Jones et al., 2016). Abrupt contacts signify episodes of high rates of interdune erosion by the dunes, which generated laterally extensive interdune bounding surfaces (see above detailed description and interpretation of these bounding surfaces in section 5.1) (Kocurek, 1981; Kocurek 1988).

6. PRECAMBRIAN LINEAR MEGADUNES: SEDIMENTOLOGICAL FEATURES AND THEIR IMPLICATIONS FOR THE MORPHOLOGICAL RECONSTRUCTION

To reconstruct the primary dune morphology from the cross-strata assemblages and their sedimentary features, three main criteria were considered: (i) the sedimentary facies, (ii) the interplay

between megadune and inter-megadune strata, and (iii) the geometrical relationships between cross-strata and bounding surfaces. These are discussed next based on field observations and complemented by the current knowledge about linear megadunes.

6.1. The sedimentary lithofacies

The foremost criteria for the reconition of linear megadune deposits within aeolian successions is the stratigraphic relationship of the distinct aeolian lithofacies, as proposed by Clemmensen (1989) and Chrintz and Clemmensen (1993). This model is based on the internal structures formed during the construction and migration of linear megadunes. Studies of ancient and current aeolian systems have demonstrated that there are different arrangements of these lithofacies, which are related to two main morphodynamic stages: (i) vertical accretion and (ii) lateral migration phases (Fig. 2) (cf. Clemmensen, 1989; Yu et al., 2021). Both stages are identified from the studied depositional architecture.

The compound arrangement of sets of cross-strata records the development of superimposed migrating dunes atop a larger bedform (megadunes). These deposits are commonly generated and accumulated in the central part of the megadunes during their migration (Clemmensen, 1989). The gradational contacts observed between the megadune foresets and the "low-angle cross-bedded sets" downwind suggest a well-developed plinth sedimentation at the lowermost part of mega-bedform. In addition, the unusual thickness of plinth strata suggests low rates of cannibalisation of plinth deposits by advancing megadunes, thereby demonstrating the construction of megadunes under (i) low sand drift rates towards lee slope direction and (ii) considerable rates of aggradation of the plinth packages. These features are common in linear megadunes during the development of the vertical accretion stage, which is characterised by high rates of growth and longitudinal elongation produced by the sand drift oblique or perpendicular to the megadune lee slope (Tsoar, 1989; Bristow et al., 2005). In this vertical accretion phase, the dune elongation resulting from parallel sand drift along the dune crestline reduces the likelihood of plinth strata destruction by the primary airflow during the bedform migration (Lancaster, 1982; Livingstone, 1989; Tsoar et al., 2004; Rubin et al., 2008) (Fig. 11A). The significant sand supply that may

have characterised many Precambrian aeolian systems, together with a regular bimodal wind-pattern circulation, probably facilitated the accretion of protodunes while maintaining their linear and symmetrical shapes (e.g., Lancaster, 1982; Tsoar, 1989; Dong et al., 2004) (Fig. 11A).

The well-development of plinth deposits is also evident in modern transverse megadunes (Havholm and Kocurek, 1988). Yet, these deposits are often not preserved in the long term due to two primary factors: (i) turbulent winds, which are generated in front of the megadune leeside due to the slightly oblique orientation of primary airflows relative to the slipface, leading to the removal of sand from the plinth deposits, and (ii) rapid migration rates of transverse megadunes, which act to limit the time for the accumulation of thick plinth deposits and conversely facilitate their erosion during bedform migration (Kocurek, 1986; Besler, 2000; Mountney, 2006; Langford et al., 2008). Consequently, commonly only relatively thin low-angle-inclined plinth strata are preserved as the toesets of transverse dune cross-strata (< 2 m thickness) (cf. Mountney and Thompson, 2002; Mountney and Jagger, 2004; Mountney, 2006b).

During the lateral migration phase, the lithofacies associated with the central megadune, lower plinth, and inter-megadune regions tend to become vertically stacked (Fig 11B). Sideways movement may lead to the partial erosion of the deposits adjacent to the larger bedform (i.e., plinth deposits) due to sediment removal by turbulent winds acting in front of the megadune lee slope oriented toward the lateral sand-drift direction. As the depositional system shifts laterally, so the linear mega-bedforms develop an asymmetrical profile, marking the onset of their lateral migration phase.

The irregular or undulated first-order type A bounding surface that sharply delineates the compound cross-bedded and low-angle cross-bedded sets comprises the basic depositional architecture produced by the lateral migration of linear megadunes over adjoining inter-megadune corridors during their lateral migration phase. Similar features and interpretations have been observed by Clemmensen (1989) and Chrintz and Clemmensen (1993) in the Lower Permian Yellow Sands (Northeast England), Scherer (2000) in the Cretaceous Botucatu Formation (South Brazil), and Besley et al. (2018) in the Permian Auk Formation (North Sea). The analysed succession exhibits at least two sequences of inter-megadune and lower megadune plinth-central megadune deposits, which are separated by erosional first-order bounding

surfaces (Figs. 5, 6). Thus, it is possible to suggest that this lithofacies organisation reflects an early phase of vertical accretion succeeded by lateral migration of two linear mega-bedforms migrating over wide and large inter-megadune corridors (Fig. 11A, B).

In summary, the gradational contact between the foresets of sets composed of cross strata (central megadune deposits) and plinth strata, in addition to the unusual thicknesses of these deposits (several metres), are indicative of linear mega-bedforms deposits in their vertical accretion phase. By contrast, the successive stacking of these facies, delimited by extensive first-order type A bounding surfaces, suggests lateral migration of this linear megadune system (Clemmensen, 1989, Fig. 10).

6.2. The relationships between megadune and inter-megadune deposits

Inter-megadune deposits are rarely recognised or well-preserved in most megadune successions, primarily due to their susceptibility to be completely eroded during the mega-bedform migration. Thereby, their long-term accumulation is commonly hampered (Kocurek and Havholm, 1993; Kocurek and Day, 2018). The erosion of inter-megadune strata in the megadune systems is heavily influenced by two main factors: (i) the style of megadune migration, and (ii) the absence of agents promoting the sand accumulation in dry environments.

First, megadunes usually migrate at a negative to a very low but positive angle of climb, enhancing the risk of erosion of the adjoining interdune flats during migration (Mountney and Howell, 2000; Mountney, 2012; Rodríguez-Lopez et al., 2014). Moreover, in aeolian systems characterised by high dune migration rates, inter-megadune deposits are rapidly consumed (Mountney, 2012), hindering the formation of thick deposits, which would decrease their chances of accumulation after the passage of the mega-scale bedform (Mountney and Thompson, 2002; Mountney 2006b; Mesquita et al., 2021b).

Second, based on evidence from the Phanerozoic record and current observations, the extensive construction of mega-bedforms appears to be confined to hyperarid environments (Scherer, 2000; Al-Masrahy and Mountney, 2013; Pye and Tsoar, 2009). It occurs because the effective construction of

586 megadunes requires a large amount of sand available for the transport and sedimentation by the wind,
587 predominantly found in desert landscapes (Wilson, 1973; Porter, 1986; Mountney, 2006). In these
588 environments, the water table and its capillary fringe typically remain well below the accumulation surface,
589 making interdune strata highly susceptive to erosion by migrating bedforms. The absence of other factors
590 controlling sand accumulation (e.g., vegetation, soils) facilitates effective sand removal by the wind
591 (Havholm and Kocurek, 1994). Thus, interdune strata often undergo complete erosion in dry aeolian
592 systems, resulting in the formation of large first-order bounding surfaces within the preserved depositional
593 architecture (Kocurek, 1991, Langford et al., 2008; Basilici et al., 2021, Fig. 7).

594 However, this conceptual model does not explain the processes of construction and accumulation
595 that have been inferred for dry inter-megadune deposits of the Galho do Miguel Formation. Indeed the
596 "planar-parallel sandstone strata" element (dry-interdune deposits) exhibits unusual thicknesses of up to
597 6 m and lateral extensions reaching 100 m and is repeatedly interbedded and/or laterally connected with
598 "compound cross-bedded sets" element (megadune deposits) (Figs. 5, 6).

599 The absence of terrestrial vegetation allowed the temporary accumulation of aeolian sands, except
600 in cases where sand accumulation was influenced by a near-surface water table (Basilici et al., 2021).
601 Recent studies have discussed how dry-interdune deposits could also be accumulated in areas with a
602 high groundwater level, provided that this does not impact dry aeolian sedimentation significantly. Due to
603 the proximity of the water table to the depositional surface, dry interdune flats may experience erosion
604 only up to the groundwater level. At this interface, the presence of moisture would impede sand removal
605 during dune migration, resulting in simultaneous accumulation of climbing dune and dry interdune strata
606 (Havholm and Kocurek 1988; Mesquita et al., 2021b).

607 A second potential controlling factor considers the pattern aeolian sedimentation throughout the
608 Proterozoic era. The barren surface of Precambrian continents likely experienced higher rates of erosion
609 and weathering compared to the post-vegetation Earth, leading to the generation of a substantial sediment
610 supply, much of which was available for wind transport (Bose et al, 2012). These conditions, coupled with
611 the prevalent sand-supersaturated sediment wind flows, likely resulted in the widespread formation of

larger aeolian systems (Eriksson and Simpson, 1998; Eriksson et al., 2005; Bose et al., 2012; Cosgrove et al., 2023). This palaeoenvironmental condition allowed high rates of sedimentation into inter-megadune flats, which, hence, provided a high accretion rate of the inter-megadune substrate leading to deposits of notable thickness. In this regard, it is sensible to infer that the migrating megadunes were likely unable to rework all the sand accumulated in dry interdune areas, resulting in the climbing of dune and interdune forms over time (cf. Basilici et al., 2021; Mesquita et al., 2021b). These palaeoenvironmental conditions facilitated relatively high rates of sedimentation in interdune flats, thereby reducing the erosive potential on the interdune substrate and promoting substantial accumulation of deposits (cf. Basilici et al., 2021; Mesquita et al., 2021b).

Moreover, the scale and morphology of the original migrating bedforms may have also influenced the thicknesses of the preserved inter-bedform strata. Megadunes require a substantial sand supply for their formation and continued construction and maintenance, thereby promoting the deposition and accumulation of thick sand packages in adjacent inter-megadune flats (Pye and Tsoar, 2009; Mountney, 2006b). During the accretion stage, the predominant elongation of the linear megadunes allows the formation of extensive inter-megadune corridors between these bedforms (Munyikwa, 2005; Lucas et al., 2015; Davis et al., 2020). At times of slow lateral migration associated with dominant vertical accretion, the sediments deposited within these corridors typically experience partial erosion by wind deflection, leading to their gradual aggradation (Tsoar, 1983; Rubin, 1990; Rubin et al., 2008) (Fig. 11).

Based on examples of Martian aeolian systems, which serve in some ways as approximate modern analogues to Precambrian Earth, the erosion of inter-megadune flats due to lateral migration of linear megadunes is comparatively slower than that observed in systems with mobile transverse megadunes (Bouke et al., 2010; Reffet et al., 2010; Davis et al., 2020). This characteristic is attributed to the predominant longitudinal growth of linear bedforms, which limits their lateral mobility (Tsoar, 1983; Rubin et al., 2008). Consequently, this prevailing feature naturally provides the heightened development of dry inter-megadune deposits, which are accumulated over the long term through climbing processes (Fig. 11) (Mountney and Thompson, 2002; Mountney, 2012).

638 The depositional architecture suggests that the linear megadune system of the Galho do Miguel
639 Formation experienced both development phases (vertical accretion and lateral migration stages – Fig.
640 2). The encroached and gradual contacts between inter-megadune strata and the dune toe-sets are
641 indicative of low rates of megadune migration over inter-megadune areas, as well as of a low rate of
642 interdune reworking, providing the partial erosion of these strata by mega-bedform advance. The contacts
643 also suggest a lateral coexistence and coeval accumulation of linear megadunes and inter-megadune
644 deposits over time, which suggests synchronous migration of dunes and adjoining interdunes (Fig. 11)
645 (Pulvertaft, 1985; Mountney, 2006b; Jones et al., 2016; Mesquita et al., 2021b). The presence of vortex-
646 ripple marks close to megadune slipfaces indicates seasonal oscillation of a near-surface water table,
647 which must have contributed to the retention of sand in inter-megadune corridors during megadune
648 advance (Jones et al., 2016; Mesquita et al., 2021a). Therefore, it can be inferred that the accumulation
649 of dry inter-megadune deposits was likely intimately linked to the process of construction of the linear
650 megadunes.

651

652 **6.3. The reconstruction of megabedform assemblages from compound cross-strata**

653 The construction of a mega-scale bedform involves complex mechanisms of superimposition,
654 migration, and climbing of the larger bedform and its parasitic dunes. These processes are ruled by the
655 interplay of different controlling factors, such as (i) the wind-pattern circulation and the resultant sand drift;
656 (ii) morphometric elements of the migrating dune (i.e., the crestline sinuosity, the leeside height, the
657 direction of the dune crestline concerning the effective airflow); (iii) the wind velocity and saturation with
658 respect to its potential sand-transport capacity; (iv) the type of aeolian system (i.e., wet, dry, or stabilised
659 aeolian system); and (v) the original dune topography (McKee, 1979; Montney, 2006a; Pye and Tsoar,
660 2009). These same factors also act to control the geometric characteristics of the deposits, chiefly in
661 relation to the morphodynamic behaviour of the main bedform (e.g., longitudinal or transversal). The
662 following discussion attempts to relate the geometrical relationship between the cross-strata and
663 bounding surfaces with the conditions of development and construction of a complex linear megadune.

Some of these relationships were explored previously via the computational models of Rubin and Carter (2006).

A fundamental diagnostic element for the recognition of megadune deposits in ancient successions is the compound arrangement of the cross-strata. Unlike deposits originated by simple transverse dunes, the dip of these cross-strata does not correspond with the resultant direction of migration of the main bedform. Instead, the orientation of the superimposition surfaces is expected to be indicative of the megadune orientation, assuming that these surfaces originated in a perpendicular orientation to the megadune brink line, whereas the cross-strata are formed by the smaller and superimposed dunes that migrate over the megadune slipface (Havholm and Kocurek, 1988). Studies of modern ergs suggest that the overall orientation of a megadune is determined by the average wind-pattern circulation. In contrast, the superimposed bedforms are oriented according to either secondary airflows over downslopes (cf. Havholm and Kocurek, 1988) or turbulent winds operating in front of the large leeside (cf. Lancaster, 1982), resulting in a large variety of dune morphologies (e.g., oblique, transversal, or linear dunes according to the multidirectional pattern of the resultant winds) (Havholm and Kocurek, 1988; Pye and Tsoar, 2009). Thus, in linear mega-bedforms, the orientation of the main crestline is dictated, in the long term, by the bimodal primary winds responsible for the dune elongation process. The smaller superimposed dunes can be expected to migrate systematically in a direction that aligns with the overall megadune crest or in a possible angular component, which is more likely due to the complexity of the wind circulation (Pye and Tsoar, 2009; Davis et al., 2020). This relationship implies a high angularity of the main trend of the dune superimposition direction and of the orientation of the linear megadune slipfaces with respect to the mean orientation of the megadune crestline. Evidence to demonstrate this in preserved stratal successions is derived from the spatial relationship between the dip-azimuths of the foresets and the superimposition surfaces. Computational models proposed by Rubin and Carter (2006, Fig. 56 and Yan et al., 2024) support this idea.

This geometrical relationship is often recognised throughout the deposits of the Galho do Miguel Formation and is taken as evidence of the activity of a complex linear megadune system. At the Morro do

690 Batatal locality (Fig. 1C), the average value of foreset dip azimuths is towards c. 60°, whereas the
691 superimposition surface dip azimuths are dominantly towards c. 115° (Figs. 5D, E). At the Serra do
692 Pasmar locality (Fig. 6D, E), the main palaeodirection of dune foresets is towards c. 80°, whereas the
693 superimposition surfaces dip towards c.145°. These relationships suggest a set of oblique dunes
694 migrating over the megadune flank at an angle <20°, concerning the megadune lee-slope. Based on the
695 stereo-net reconstruction techniques proposed by Rubin and Hunter (1983, their Table 1), the directions
696 of dune superimposition in both situations were, on average, towards 100° and 127°. These values
697 indicate superimposed oblique dunes that migrated at an clockwise angle of more than 40° concerning
698 the main direction of the megadune flanks (Hunter et al., 1983; Clemmensen and Blakey, 1989; Rubin,
699 1990) (Fig. 13). The high spread of dip-azimuths of the superimposition surfaces might be due to the high
700 sinuosity of the megadune crestlines and/or the high morphological complexity of superimposed dunes
701 (Brookfield, 1977; Havholm and Kocurek,1988; Kocurek, 1981a; Mountney, 2006a). This argument is
702 supported by two additional pieces of evidence. First, the high spread of the dip azimuths of plinth cross-
703 strata, because these are generated in a direction that is nearly parallel to the megadune lee faces by
704 avalanche processes, and they tend to be oriented according to the original morphology of the dune (Fig.
705 13) (Rubin, 1987; Scherer, 2000; Mountney and Howell, 2000). Second, the slight obliquity (<25°)
706 between the main values of dip-azimuth of plinth cross-bedding (120°) and superimposition surfaces
707 (145°), which may also be a product of the high sinuosity of the megabedforms (Lancaster, 1982; Rubin
708 and Hunter, 1983; Havholm and Kocurek,1988; Mesquita et al., 2021).

709 In this study, the direction of dune superimposition may be close to the main resultant sand drift
710 direction, which occurred oblique clockwise (c. 40°) to the mean trend of the cresltine of the linear
711 megadune (c. 030º azimuth). This arrangement is common in the modern linear megadunes developed
712 in sand seas (Fig. 13) (Lancaster, 1982; Havholm and Kocurek,1988; Pye and Tsoar, 2009). In contrast,
713 in transverse megadune systems, even though the angle between the megadune crestline and the
714 direction of dune superimposition tends to be high (>60°), the angle between the foreset dip azimuths of
715 superimposed dune and the megadune slope surfaces tends to be low (<20°), since the directions of

716 mega-bedform migration and dune superimposition are similar and parallel to the unidirectional airflow
717 (Scherer, 2000; Mountney, 2006a; Langford et al., 2008). In this context, plinth cross-strata foresets are
718 dominantly oriented according to a similar direction (or at very low angle) to the migration of superimposed
719 dunes, unlike in linear megadune systems (Havholm and Kocurek,1988; Scherer, 2000; Mountney and
720 Thompson, 2002; Mountney, 2006a).

721 The apparent bidirectional trend of the foresets, as evidenced by a plot of poles to the
722 superimposed surfaces observed in the Serra do Pasmar deposits (Figs. 1B, 4E), suggests the
723 development of mega-bedforms with two main slip faces (Chrintz and Clemmensen, 1993). This feature
724 is strong evidence of the construction of linear megadunes. However, the local occurrence of this feature
725 (c. 15% of the total analysed succession) might indicate the initial stage of megadune aggradation during
726 the vertical accretion phase, followed by a generalised lateral migration of this system.

727 Considering that the palaeomigration direction of oblique dunes is not parallel to the megadune
728 crestline, it can be suggested that the main sand drift direction was not parallel to the crestline of this
729 linear megadune system (cf. Clemmensen and Blakey, 1989; Bristow et al., 2005; Rubin et al., 2008).
730 Over time, this condition will have facilitated the development of a net sideways shift, with megadunes
731 moving laterally at a slower rate compared to their longitudinal growth (Tsoar et al., 2004; Rubin and
732 Hunter, 1987). This corroborates the hypothesis of lateral bedform drift and the onset of a lateral migration
733 phase within the studied system. This migrating component was likely responsible for (i) the processes of
734 cannibalisation and accumulation of adjoining interdune deposits, (ii) the stacking style of the sedimentary
735 facies, and (iii) the loss of the bimodal pattern of dune cross-strata.

736

737 **7. PRECAMBRIAN LINEAR MEGADUNES: CONTROLLING FACTORS**

738 Based on the reconstruction of the palaeodunes of the Galho do Miguel Formation and the peculiar
739 environmental conditions prevalent on Precambrian landmasses, the following discussion considers (i)
740 the process of megadune construction, (ii) the mechanisms that likely controlled the accumulation and

741 preservation of ancient linear megadune systems, and (iii) similarities and differences between
742 Proterozoic and Phanerozoic linear megadunes.

743

744 **7.1. Megadune construction: depositional model, palaeowind circulation and morphodynamics**

745 The aeolian system of the Galho do Miguel Formation comprises linear megadunes composed by
746 superimposed dunes with a high morphological variety (Fig. 12). The thickness and usual interstratification
747 of dry inter-megadune element with megadune element deposits suggest the presence of large and well-
748 developed inter-megadune corridors between the megabedforms (Chrintz and Clemmensen, 1993;
749 Abrantes Jr et al., 2020). These inter-megadune areas are also thought to have accommodated smaller
750 dune fields, composed of transverse or crescentic dunes. It is likely that these simple dunes fields
751 migrated and climbed over smaller interdune flats (Fig. 12). The limited thickness of sets of simple dune
752 elements (up to 2 m think) and their local association with the thick deposits of planar-parallel sandstone
753 strata (dry inter-megadune element) (Fig. 3) support this interpretation. Additionally, the depositional
754 architecture of the simple dune elements is interpreted to reflect the construction of dunes that were up
755 to 15 m high and that migrated towards c. 080° across these smaller interdune flats. The drift direction of
756 these simple dunes was similar to the lateral palaeotransport direction of the linear megabedforms: this
757 suggests a more persistent regional wind direction towards the NE in a bimodal wind circulation, probably
758 coupled with less effective wind transport towards the NW. This wind pattern is commonly observed in
759 present-day linear megadune systems (Wang et al., 2004). In this palaeoenvironment, the absence of
760 water likely allowed the complete erosion of interdune deposits, leading to the formation of large interdune
761 surfaces during dune climb.

762 The Galho do Miguel Formation is constituted of the deposits of complex linear megadunes (Fig.
763 12). Given the bimodal wind-circulation pattern necessary for dune construction and for maintaining their
764 morphology, a mean direction of sediment transport in a direction parallel to the dune crest (i.e., oriented
765 <15° from the sand ridge) is envisaged (cf. Tsoar et al., 2004; Besler, 2000; Davis et al., 2020). In this
766 system, the net sand-moving capacity tends to be low due to the multidirectional wind regime, which

767 inhibits direct and fast sand transport across the megadune crestline (cf. Wilson, 1971; Fryberger, 1979).
768 Thus, the sediment remains in the system for a much longer time compared to fields of transverse dunes
769 controlled by unidirectional winds; over time and under an adequate sand supply, this causes bedform
770 aggradation and the superimposition of dunes (Wang et al., 2004; Mountney 2006a; Lucas et al., 2015).

771 During the vertical accretion stage, the palaeodirection of superimposed dune migration tends to
772 be governed by the elongation drift, and to be oriented slightly oblique to the dune crestline on average
773 (Fig. 12) (Lancaster, 1982; Besler, 2000; Rubin and Carter, 2006). Thus, the mega-bedform crestline, as
774 well as the sand drift during the aggradation stage, appears to have been oriented mostly towards NE
775 (Fig. 12). The high sediment supply that may have been typical during Precambrian times likely favoured
776 high rates of bedform growth for Proterozoic megadunes, compared with Phanerozoic examples.

777 In the lateral migration stage of development, the megadune starts to migrate sideways and,
778 consequently, the bimodal pattern of cross-strata orientation becomes overprinted, as observed in the
779 Galho do Miguel deposits. The accumulated deposits tend to be preferentially oriented according to the
780 lateral migration direction. Therefore, as the plinth deposits are mostly oriented in this direction, and
781 perpendicular or oblique to the crest line (Rubin, 1990, Chrintz and Clemmensen, 1993), it is inferred that
782 the studied linear megadune system migrated laterally toward SW (Figs. 12, 13).

783 Research on modern megadune systems suggests that primary airflows, crucial for sand drift along
784 megadune lee flanks, may be deflected by their interaction with the mega-bedform topography, generating
785 secondary airflows and/or turbulent winds operating in front of the lee slopes (Havholm and Kocurek,
786 1988). The linear megadunes described herein were likely originated from a dual distribution of the
787 effective winds, responsible for their elongation, whereas the secondary airflows contributed to the
788 formation of parasitic dunes of varied morphologies (e.g., oblique, transversal, or linear dunes depending
789 on the multidirectional nature of resultant winds) migrating over megadune slope surfaces towards NE
790 (Havholm and Kocurek, 1988; Davis et al., 2020). Given that the ridge orientation is approximately 30° to
791 40° relative to the direction of the main prevailing winds, it is plausible that the airflows blew predominantly

792 to NE and NW throughout the year (see Figs. 12, 13) (cf., Besler, 2000; Tsoar, 2001). This interpretation
793 is also supported by the sand drift palaeodirection data of simple dunes.

794

795 **7.2. Bedform climbing and processes of accumulation**

796 Despite a positive net sediment budget supporting the development of linear megadunes, the sand
797 drift rate in this system is low (Mountney, 2006b). This rate is even lower than that of simple or compound
798 transverse dunes (cf. Wilson, 1971; Fryberger, 1979). Consequently, the sand remains in the system
799 longer, leading to high rates of vertical accretion and reduced migration rate (Wilson, 1971; Mountney,
800 2006b). The limited migration of these megadunes implies that high climbing angles are not expected,
801 likely approaching zero or even displaying a negative trend (Mountney, 2012; Rodríguez-Lopez et al.,
802 2014).

803 Even though these dunes might migrate sideways, theoretically allowing their climbing over inter-
804 megadune flats, the angles of climb are typically low. This observation is supported by the
805 palaeoenvironmental reconstruction performed on the linear megadune deposits of the Low Permian
806 Yellow Sandstones, where climbing angles were estimated to be less than 0.15° (Clemmensen, 1989).
807 This morphodynamic pattern elucidates the apparent absence of megadune deposits in the Precambrian
808 record, given that these bedforms migrate at a very low angle of climb, resulting in the accumulation of
809 thin beds preserving the lowermost part of these large bedforms (e.g., the plinth deposits - Rodríguez-
810 Lopez et al., 2014).

811 Conversely, the sedimentary features of the Galho do Miguel Formation suggest the influence of
812 multiple factors in governing sand accumulation, in contrast with depositional models based on
813 Phanerozoic examples. The remarkable thickness and relatively high preservation of linear megadunes
814 and inter-megadune deposits (comprising successions up to 60 m thick) suggest that this system might
815 have undergone aeolian accumulation through mechanisms other than climbing, although this process of
816 accumulation may still have been dominant in this dry aeolian environment. The encroached and

817 gradational contacts between the cross-strata and inter-megadune deposits imply synchronous
818 accumulation and coeval climbing of megabedforms over adjoining inter-megadune flats (cf. Pulvertaft,
819 1985; Mountney, 2012; Mesquita et al., 2021b). This process often occurs over high angles of climb,
820 which are uncommon in dry aeolian systems (Mountney and Thompson, 2012; Mountney, 2012).

821 Although the climbing process does not contribute to the accumulation of thick inter-megadune
822 deposits in dry environments (Mountney and Jagger, 2004; Mountney, 2012), it apparently played a
823 crucial role in the accumulation of linear megadunes of the Galho do Miguel Formation. The apparent
824 contradiction in the accumulation pattern of these megadunes, as well as the lack of deposits indicating
825 exceptional accumulation and preservation mechanisms (such as those covered by lava flows or deposits
826 consequence of sea level transgressive events), raise the following questions: (i) how was the
827 accumulation of thick megadune strata possible through climbing in the ancient dry aeolian systems? Was
828 this process unique to Precambrian aeolian systems? A possible answer to these questions lies in the
829 coupled influence of the water-table level and the sedimentary condition of Precambrian aeolian
830 environments.

831 In this dry aeolian system, the water-table level must have remained beneath the accumulation
832 surface almost constantly. Nevertheless, sedimentological evidence is seen (e.g., the occurrence of
833 vortex ripple-marks and the geometry of the first-order type A bounding surface) of a seasonal influence
834 of the water table (or its capillary fringe) on the accumulation surface. Under conditions of high sediment
835 supply and high aggradation rates, as observed during the vertical accretion stage of these linear
836 megadunes, the distribution of wet features throughout the examined succession implies a gradual rise
837 in the water-table level, which probably followed the elevation of the dry substrate. Additionally, the
838 variation of climbing angles of mega-bedforms during migration, as testified to by the geometry of inter-
839 megadune deposits, suggests seasonal changes in airflow saturation and velocity (Mountney, 2012;
840 Mesquita et al., 2021). These fluctuations might be associated with cyclic periods of wetter depositional
841 surfaces caused by water-table fluctuations. The adhesion of sand to the wet substrate also hinders sand

842 reworking by advancing megadunes, altering the inter-megadune cannibalisation rates and producing
843 different geometries of their strata (Mountney, 2012; Mesquita et al., 2021).

844 Therefore, during megadune climb, the water table might have also indirectly acted as an additional
845 factor in the accumulation of these strata. Due to the proximity of the water-table level to the dry
846 accumulation surfaces, the inter-megadune deposits were only eroded up to the groundwater level, where
847 wetness prevented the sand removal by the migration of the succeeding bedform (Fig. 11). In this system,
848 the water table rarely reached the accumulation surface due to the high rate of aggradation of the dry
849 substrate that is expected in relation to the high volume of windblown sand that will have been typical in
850 the Precambrian (Fig. 11). These conditions are likely to have driven the coeval accumulation of linear
851 megadune and dry inter-megadune deposits in the long term, despite the widespread absence of sand-
852 fixing agents in Precambrian times.

853 The high sand supply in Precambrian times must have facilitated the production of linear
854 megadunes with higher lateral migration rates and aggradation rates, compared to Phanerozoic
855 equivalents. Therefore, it is possible to propose that the long-term accumulation of thick deposits of the
856 Galho do Miguel aeolian system could only exist owing to the environmental condition that ruled the
857 Precambrian ergs combined with the action of the water table.

858

859 **7.3. Similarities and differences between Proterozoic and Phanerozoic linear megadunes**

860 The depositional architecture of the Galho do Miguel Formation is not entirely consistent with
861 depositional models based on Phanerozoic examples (Mountney, 2012; Rodríguez-López et al., 2014 –
862 see their Fig. 3). It is likely that this reflects the different mechanisms of sand accumulation and the unique
863 palaeoenvironmental aeolian processes of Precambrian ergs.

864 Recent research attributes the water table as the main agent of aeolian accumulation in
865 Precambrian aeolian systems (Bállico et al., 2017; Basilici et al., 2020, 2021). In the pre-vegetated Earth,
866 extensive megadunes likely dominated the dry landscape. Nevertheless, without sand-stabilizing agents,

867 such as vegetation, exogenous agents (e.g., wind, rivers, and sea waves) were able to rework the
868 accumulated deposits and hinder their preservation (Tirsgaard and Øxnevad, 1998; Simpson et al., 2002;
869 Lebeau and Ielpi, 2017; Heness et al., 2014). On the contrary, in wetter palaeoenvironmental conditions,
870 the water table lay near or at the accumulation surface, binding the sand grains together and blocking
871 their removal by erosional agents (Basilici et al., 2020; 2021). This accounts for the widespread presence
872 of wet aeolian systems in the Precambrian sedimentary record, differing from the Phanerozoic record,
873 where aeolian systems tended to develop and accumulate predominantly in arid or semi-arid climates
874 (Cosgrove et al., 2023, Fig. 5). This contrast is attributed to greater sediment supply in the Precambrian
875 times, which likely facilitated substantial dune construction, even in the presence of moist substrates that
876 would otherwise inhibit sediment availability and aeolian bedform development (Mountney and
877 Thompson, 2002, Mountney, 2006a; Mountney, 2006b).

878 The greater availability of sand in most Precambrian ergs may not have specifically favoured the
879 formation of linear megadunes, since these bedforms develop mainly on large deflation surfaces with
880 limited sand availability (Mainguet and Chemin, 1983). However, in aeolian systems influenced by water-
881 table fluctuations, the sand available for wind transport tends to be reduced due to the seasonal formation
882 of wet surfaces in inter-megadune areas. In this case, the water table can influence the construction and
883 maintenance of this megadune systems indirectly, by controlling the amount of sand that feeds dune
884 superimposition in a linear mega-bedform system and long-term sand accumulation. This set of factors
885 could explain the exceptional development and accumulation of linear megadunes in the studied system
886 and the apparent scarcity of these deposits in the Precambrian record overall. This scarcity was previously
887 proposed by Cosgrove et al. (2023).

888 To conclude, the unusual thickness of compound cross-stata of linear megadune origin in the Galho
889 do Miguel Formation appears to be related to the interplay of particular palaeoenvironmental conditions
890 of the Precambrian time and to a high water table. This suggests that large-scale bedforms likely formed
891 extensively in the Precambrian continents, even in wet/damp climates (cf. Cosgrove et al., 2023). Yet, in

dry environments they were only temporally accumulated due to the absence of sand-fixing agents for long-term accumulation, (Basilici et al., 2021; Mesquita et al., 2021b).

8. CONCLUSIONS

The depositional architecture of the Galho do Miguel Formation portrays the widespread development of megadunes (or draas). This system is interpreted as composed of complex linear megadunes surrounded by extensive dry inter-megadune areas and small fields of simple transverse dunes. According to the architectural analysis of the aeolian succession of the Galho do Miguel Formation, it was possible to make the following considerations:

(i) Although the preservation of primary megadune topography is a common criterion for recognising linear mega-bedforms in ancient successions, this study demonstrates that the depositional architecture can be useful to identify dune morphology when the original topography is not preserved. Three criteria were used to differentiate the studied linear megadunes from transverse megabedform deposits: (i) sedimentary facies, (ii) relationships between megadune and inter-megadune strata, and (iii) the geometrical relationships between cross-strata and bounding surfaces.

(ii) The linear megadune system underwent two distinct stages of development: vertical accretion and lateral migration. During the vertical accretion stage, the typically high sediment supply of the Precambrian and the bimodality of the primary flow promoted higher rates of mega-bedforms growth, their elongation through longitudinal sand drift, and the formation of superimposed dunes. The linear megadunes also migrated laterally, facilitating the erosion of deposits associated with the secondary megadune slipface opposite to the direction of lateral migration. Thus, the accumulated cross-strata have unimodal cross-bed dip directions, resembling deposits of transverse megadunes. The studied deposits revealed dominant lateral migration towards SE and a main direction of superimposition by oblique dunes towards NE.

(iii) However, the thickness and remarkable preservation of the depositional architecture of this linear megadune system suggest different mechanisms of sand accumulation for Precambrian ergs. Some sedimentary features indicate that the process of megadune climb, and the aggradation of the accumulation surface occurred coevally to a progressive rise of the water-table level. Since it is likely that the water table remained below the accumulation surface most of the time, it may not have influenced the dry sedimentation of this aeolian system but may still have prevented complete sand removal by migrating megadunes and other exogenous agents (e.g., wind, rivers, sea waves).

(iv) This paper demonstrates that the accumulation of dry inter-megadune deposits were more likely to occur in Precambrian settings due to two primary factors. (i) The elevated rates of inter-megadune substrate aggradation resulting from higher sediment supply coupled with a progressive rise of the water table. (ii) The slower lateral migration of megadunes relative to their longitudinal growth, resulting in lower sand removal rates from the adjacent inter-megadunes during bedform climb. Over time, these inter-megadunes accumulated concurrently with compound cross-strata, potentially offering compelling evidence for identifying linear mega-bedforms in the ancient geological record.

(v) The scarcity of linear megadune deposits in Precambrian ergs might be linked to: (i) misidentification of their deposits, and/or (ii) environmental conditions of Precambrian aeolian environments that were not conducive to their construction and accumulation.

ACKNOWLEDGEMENTS

The authors thank the National Agency of Petroleum, Natural Gas and Biofuels of Brazil (ANP) and the PRH-ANP 19.1 (Programa de Formação de Recursos Humanos em Exploração Petrolífera e Geologia de Reservatórios) for the financial support and grant to the first author (grant n. 042919/2021 of A.F.M), CNPq (Research Grant 309767/2022-9 of C.R.S.F) and FAPESP (2017/03649-9 of G.B.). We also thank the Casa da Glória team (Federal University of Minas Gerais), Mr. Geraldo Damaso, and Lady Silvia de Oliveira for their support during the fieldwork.

REFERENCES

Abrantes Jr, F.R., Basilici, G., Soares, M.V.T., 2020. Mesoproterozoic erg and sand sheet system: Architecture and controlling factors (Galho do Miguel Formation, SE Brazil). Precambrian Research 338, 105592. https://doi.org/10.1016/j.precamres.2019.105592

Ahlbrandt, T.S., Fryberger, S.G., 1981. Sedimentary features and significance of interdune deposits.In: F.G. Ethridge, R.M. Flores (Eds.), Recent and Ancient Nonmarine Depositional Environments: Model for Exploration. SEPM Special Publications 31, Tulsa, pp. 293-314

Allen, J.R., 1979. A model for the interpretation of wave ripple-marks using their wavelength, textural composition, and shape. Journal of the Geological Society 136, 673-682.

Al-Masrahy, M.A., Mountney, N.P., 2013. Remote sensing of spatial variability in aeolian dune and interdune morphology in the Rub'Al-Khali, Saudi Arabia. Aeolian Research 11, 155-170.

Almeida-Abreu, P.A., 1995. O Supergrupo Espinhaço da Serra do Espinhaço Meridional (Minas Gerais): o rifte, a bacia e o orógeno. Geonomos 3, 1-18 (In Portuguese with English abstract).

Bállico, M.B., Scherer, C.M.S., Mountney, N.P., Souza, E.G., Reis, A.D., Gabaglia, G.R., & Magalhães, A.J.C., 2017. Sedimentary cycles in a Mesoproterozoic aeolian erg-margin succession: Mangabeira Formation, Espinhaço Supergroup, Brazil. Sedimentary Geology 349, 1-14.

Bagnold, R.A., 1946. Motion of waves in shallow water. Interaction between waves and sand bottoms. Proceedings of the Royal Society of London - Series A - Mathematical and Physical Sciences 187, 1-18.

Basilici, G., Soares, M. V. T., Mountney, N. P., Colombera, L., 2020. Microbial influence on the accumulation of Precambrian aeolian deposits (Neoproterozoic, Venkatpur Sandstone Formation, Southern India). Precambrian Research 347, 105854. https://doi.org/10.1016/j.precamres.2020.105854

964 Basilici, G., Mesquita, Á. F., Soares, M.V.T., Janočko, J., Mountney, N.P., Colombera, L., 2021. A
965 Mesoproterozoic hybrid dry-wet aeolian system: Galho do Miguel Formation, SE Brazil. Precambrian
966 Research 359, 106216. https://doi.org/10.1016/j.precamres.2021.10621

967 Besler, H., 2000. Modern and palaeo-modelling in the Great Sand Sea of Egypt (initial results from
968 the Cologne Cooperative Research Project 389). Global and Planetary Change 26, 13-24.

969 Besly, B., Romain, H.G., Mountney, N.P., 2018. Reconstruction of linear dunes from ancient
970 aeolian successions using subsurface data: Permian Auk Formation, Central North Sea, UK. Marine and
971 Petroleum Geology 91, 1-18.

972 Blakey, R.C., 1988. Basin tectonics and erg response. Sedimentary Geology 56, 127-151.

973 Bose, P.K., Eriksson, P.G., Sarkar, S., Wright, D.T., Samanta, P., Mukhopadhyay, S., Mandal, S.,
974 Banerjee, S., Altermann, W., 2012. Sedimentation patterns during the Precambrian: A unique record?
975 Marine and Petroleum Geology 33, 34-68.

976 Bourke, M.C., Lancaster, N., Fenton, L.K., Parteli, E.J., Zimbelman, J.R., Radebaugh, J., 2010.
977 Extraterrestrial dunes: An introduction to the special issue on planetary dune systems. Geomorphology
978 121, 1-14.

979 Brito Neves, B.B.D., Fuck, R.A., Pimentel, M.M., 2014. The Brasiliano collage in South America: a
980 review. Brazilian Journal of Geology 44, 493-518.

981 Brookfield, M.E., 1977. The origin of bounding surfaces in ancient aeolian
982 sandstones. Sedimentology 24, 303-332.

983 Bristow, C.S., Bailey, S.D., Lancaster, N., 2000. The sedimentary structure of linear sand
984 dunes. Nature 406, 56-59.

985 Bristow, C.S., Lancaster, N., Duller, G.A.T., 2005. Combining ground penetrating radar surveys
986 and optical dating to determine dune migration in Namibia. Journal of the Geological Society 162, 315-
987 321.

988 Bristow, C.S., Duller, G.A.T., Lancaster, N., 2007. Age and dynamics of linear dunes in the Namib
989 Desert. Geology 35, 555-558.

990 Catuneanu, O., Martins-Neto, M.A., Eriksson, P.G., 2005. Precambrian sequence
991 stratigraphy. Sedimentary Geology 176, 67-95.

992 Chemale Jr, F., Dussin, I.A., Alkmim, F.F., Martins, M.S., Queiroga, G., Armstrong, R., Santos,
993 M.N., 2012. Unravelling a Proterozoic basin history through detrital zircon geochronology: the case of the
994 Espinhaço Supergroup, Minas Gerais, Brazil. Gondwana Research 22, 200-206.

995 Chrintz, T., Clemmensen, L. B., 1993. Draa reconstruction, the Permian Yellow sands, northeast
996 England. In: K. Pye, K., Lancaster, N. (Eds.), Aeolian Sediments: Ancient and Modern. Wiley-
997 Blackwell, Oxford, UK, pp. 151-161

998 Clemmensen, L.B., 1989. Preservation of interdraa and plinth deposits by the lateral migration of
999 large linear draas (Lower Permian Yellow Sands, northeast England). Sedimentary Geology 65, 139-151.

1000 Clemmensen, L.B., Blakey, R.C., 1989. Erg deposits in the Lower Jurassic Wingate Sandstone,
1001 northeastern Arizona: oblique dune sedimentation. Sedimentology 36, 449-470.

1002 CODEMIG, 2012a. Folha Diamantina, escala 1:100000

1003 CODEMIG, 2012b. Folha Curimataí, escala 1:100000

1004 Collinson, J., Mountney, N.P., 2019. Sedimentary structures. Dunedin Academic Press, Edinburgh,
1005 UK, 320 pp.

1006 Cosgrove, G.I.E., Colombera, L. and Mountney, N.P., 2021. A Database of Aeolian Sedimentary
1007 Architecture for the characterization of modern and ancient sedimentary systems. Marine and Petroleum
1008 Geology 127, 104983. https://doi.org/10.1016/j.marpetgeo.2021.104983

1009 Cosgrove, G.I., Colombera, L., Mountney, N.P., Basilici, G., Mesquita, Á.F., Soares, M.V.T., 2023.
1010 Precambrian aeolian systems: A unique record? Precambrian Research 392, 107075.
1011 https://doi.org/10.1016/j.precamres.2023.107075

1012 Cosgrove, G.I.E., Colombera, L., Mountney, N.P., 2024. The Precambrian continental record: A
1013 window into early Earth environments. Precambrian Research 402, 107286.
1014 https://doi.org/10.1016/j.precamres.2023.107286

1015 Davis, J.M., Banham, S.G., Grindrod, P.M., Boazman, S.J., Balme, M.R., Bristow, C.S., 2020.
1016 Morphology, development, and sediment dynamics of elongating linear dunes on Mars. Geophysical
1017 Research Letters 47, e2020GL088456. https://doi.org/10.1029/2020GL088456

1018 Deynoux, M., Kocurek, G., Proust, J.N., 1989. Late Proterozoic periglacial aeolian deposits on the
1019 west African platform, Taoudeni Basin, western Mali. Sedimentology 36, 531-549.

1020 Dias, K.D.N., Scherer, C.M., 2008. Cross-bedding set thickness and stratigraphic architecture of
1021 aeolian systems: an example from the Upper Permian Pirambóia Formation (Paraná Basin), southern
1022 Brazil. Journal of South American Earth Sciences 25, 405-415.

1023 Dong, Z., Chen, G., He, X., Han, Z., Wang, X., 2004. Controlling blown sand along the highway
1024 crossing the Taklimakan Desert. Journal of Arid Environments 57, 329-344.

1025 Dussin, I.A., Dussin, T.M., 1995. Supergrupo Espinhaço: modelo de evolução
1026 geodinâmica. Geonomos 3, 19-26 (In Portuguese with English abstract).

1027 Eriksson, K.A., Simpson, E.L.,1998. Controls on spatial and temporal distribution of Precambrian
1028 eolianites. Sedimentary Geology 120, 275-294.

1029 Eriksson, P.G., Catuneanu, O., Sarkar, S., Tirsgaard, H., 2005. Patterns of sedimentation in the
1030 Precambrian. Sedimentary Geology 176, 17-42.

1031 Fryberger, S.G., 1979. Dune forms and wind regime. In: McKee ED (ed.) A study of global sand
1032 seas, Geological Survey Professional Paper, 1052. United States Geological Survey, Washington DC, pp
1033 137–169

1034 Havholm, K.G., Kocurek, G., 1988. A preliminary study of the dynamics of a modern draa,
1035 Algodones, southeastern California, USA. Sedimentology 35, 649-669.

1036 Hême de Lacotte, V.J.P. and Mountney, N.P., 2022. A classification scheme for sedimentary
1037 architectures arising from aeolian-fluvial system interactions: Permian examples from southeast Utah,
1038 USA. Aeolian Research 58, 100815, 23 pages. https://doi.org/10.1016/j.aeolia.2022.100815

1039 Heness, E.A., Simpson, E.L., Bumby, A.J., Eriksson, P.G., Eriksson, K.A., Hilbert-Wolf, H.L.,
1040 Okafor, O.J., Linnevelt, S., Malenda, H.F., Modungwa, T., 2014. Evidence for climate shifts in the~ 2.0
1041 Ga upper Makgabeng Formation erg, South Africa. Palaeogeography, Palaeoclimatology,
1042 Palaeoecology 409, 265-279.

1043 Hesp, P., Hyde, R., Hesp, V., Zhengyu, Q., 1989. Longitudinal dunes can move sideways. Earth
1044 Surface Processes and Landforms 14, 447-451.

1045 Hunter, R.E., 1977. Basic types of stratification in small eolian dunes. Sedimentology 24, 361-387.

1046 Hunter, R.E., Richmond, B.M., Rho Alpha, T.A.U.,1983. Storm-controlled oblique dunes of the
1047 Oregon coast. Geological Society of America Bulletin 94, 1450-1465.

1048 Immenhauser, A., 2009. Estimating palaeo-water depth from the physical rock record. Earth-
1049 Science Reviews 96, 107-139.

1050 Jackson, M.J., Simpson, E.L., Eriksson, K.A., 1990. Facies and sequence stratigraphic analysis in
1051 an intracratonic, thermal relaxation basin; the early Proterozoic, lower Quilalar Formation and Ballara
1052 Quartzite, Mount Isa Inlier, Australia. Sedimentology 37, 1053-1078.

1053 Jones, F.H., Scherer, C.M.S., Kuchle, J., 2016. Facies architecture and stratigraphic evolution of
1054 aeolian dune and interdune deposits, Permian Caldeirão Member (Santa Brígida Formation),
1055 Brazil. Sedimentary Geology 337, 133-150.

1056 Kocurek, G., 1981. Significance of interdune deposits and bounding surfaces in aeolian dune
1057 sands. Sedimentology 28, 753-780.

1058 Kocurek, G., 1988. First-order and super bounding surfaces in eolian sequences—bounding
1059 surfaces revisited. Sedimentary Geology 56, 193-206.

1060 Kocurek, G., 1991. Interpretation of ancient eolian sand dunes. Annual review of Earth and
1061 planetary sciences 19, 43-75.

1062 Kocurek, G., 1996. Desert aeolian system. In: H.G. Reading (Ed.), Sedimentary Environments:
1063 Processes, Facies and Stratigraphy. Blackwell Science, Oxford, UK, pp. 125-153.

1064 Kocurek, G., Dott, R.H., 1981. Distinctions and uses of stratification types in the interpretation of
1065 eolian sand. Journal of Sedimentary Research 51, 579-595.

1066 Kocurek, G., Day, M., 2018. What is preserved in the aeolian rock record? A Jurassic Entrada
1067 Sandstone case study at the Utah–Arizona border. Sedimentology 65, 1301-1321.

1068 Lancaster, N., 1982. Linear dunes. Progress in Physical Geography 6, 475-504.

1069 Langford, R.P., Pearson, K.M., Duncan, K.A., Tatum, D.M., Adams, L., Depret, P.A., 2008. Eolian
1070 topography as a control on deposition incorporating lessons from modern dune seas: Permian Cedar
1071 Mesa Sandstone, SE Utah, USA. Journal of Sedimentary Research 78, 410-422.

1072 Lebeau, L.E., Ielpi, A., 2017. Fluvial channel-belts, floodbasins, and aeolian ergs in the
1073 Precambrian Meall Dearg Formation (Torridonian of Scotland): Inferring climate regimes from pre-
1074 vegetation clastic rock records. Sedimentary Geology 357, 53-71.

1075 Livingstone, I.,1989. Monitoring surface change on a Namib linear dune. Earth Surface Processes
1076 and Landforms 14, 317-332.

1077 Loope, D.B., Simpson, E.L., 1992. Significance of thin sets of eolian cross-strata. Journal of
1078 Sedimentary Research, 62, 849-859.

1079 Lucas, A., Narteau, C., Rodriguez, S., Rozier, O., Callot, Y., Garcia, A., Courrech du Pont, S., 2015.
1080 Sediment flux from the morphodynamics of elongating linear dunes. Geology 43, 1027-1030.

1081 Mainguet, M., Chemin, M.C., 1983. Sand seas of the Sahara and Sahel: an explanation of their
1082 thickness and sand dune type by the sand budget principle. In: Brookfield, M.E., Ahlbrandt, T.S.

(Eds.), Developments in sedimentology: Eolian sediments and processes. Elsevier, Amsterdam, Netherlands, pp. 353-363.

Martins-Neto, M.A., 2000. Tectonics and sedimentation in a paleo/mesoproterozoic rift-sag basin (Espinhaço basin, southeastern Brazil). Precambrian Research 103, 147-173.

McKee, E.D., 1979. A study of global sand seas. Geological Survey Professional Paper 1052, Washington, 439 pp.

Mesquita, Á.F., Basilici, G., Soares, M.V.T., Garcia, R.G.V., 2021a. Morphology, accumulation and preservation of draa systems in a Precambrian erg (Galho do Miguel Formation, SE Brazil). Sedimentary Geology 412, 105807. https://doi.org/10.1016/j.sedgeo.2020.105807

Mesquita, Á.F., Basilici, G., Soares, M.V.T., Janočko, J., Mountney, N.P., Colombera, L., de Souza Filho, C.R., 2021b. Hybrid dry-wet interdune deposition in Precambrian aeolian systems: Galho do Miguel Formation, SE Brazil. Sedimentary Geology 425, 106007. https://doi.org/10.1016/j.sedgeo.2021.106007

Mountney, N.P., 2006a. Periodic accumulation and destruction of aeolian erg sequences in the Permian Cedar Mesa Sandstone, White Canyon, southern Utah, USA. Sedimentology 53, 789-823.

Mountney, N.P., 2006b. Eolian facies model. In: Posamentier, H.W., Walker, R.G. (Eds.), Facies Models Revisited. Special Publication of Society of Sedimentary Geology 84, Tulsa, Oklahoma, pp. 19-83.

Mountney, N.P., 2012. A stratigraphic model to account for complexity in aeolian dune and interdune successions. Sedimentology 59, 964-989.

Mountney, N.P., Howell, J., 2000. Aeolian architecture, bedform climbing and preservation space in the Cretaceous Etjo Formation, NW Namibia. Sedimentology 47, 825-849.

Mountney, N.P., Thompson, D.B., 2002. Stratigraphic evolution and preservation of aeolian dune and damp/wet interdune strata: an example from the Triassic Helsby Sandstone Formation, Cheshire Basin, UK. Sedimentology 49, 805-833.

1107 Mountney, N.P., Jagger, A., 2004. Stratigraphic evolution of an aeolian erg margin system: the
1108 Permian Cedar Mesa Sandstone, SE Utah, USA. Sedimentology 51, 713-743.

1109 Mountney, N.P., Howell, J., Flint, S., Jerram, D., 1999. Climate, sediment supply and tectonics as
1110 controls on the deposition and preservation of the aeolian-fluvial Etjo Sandstone Formation,
1111 Namibia. Journal of the Geological Society 156, 771-777.

1112 Munyikwa, K., 2005. The role of dune morphogenetic history in the interpretation of linear dune
1113 luminescence chronologies: a review of linear dune dynamics. Progress in Physical Geography 29, 317-
1114 336.

1115 Porter, M. L., 1986. Sedimentary record of erg migration. Geology 14, 497-500.

1116 Pye, K., Tsoar, H., 2008. Aeolian sand and sand dunes. Springer Science & Business Media.

1117 Pulvertaft, T.C.R., 1985. Aeolian dune and wet interdune sedimentation in the Middle Proterozoic
1118 Dala Sandstone, Sweden. Sedimentary geology 44, 93-111.

1119 Radebaugh, J., Lorenz, R., Farr, T., Paillou, P., Savage, C., Spencer, C., 2010. Linear dunes on
1120 Titan and earth: Initial remote sensing comparisons. Geomorphology 121, 122-132.

1121 Reffet, E., Du Pont, S.C., Hersen, P., Douady, S., 2010. Formation and stability of transverse and
1122 longitudinal sand dunes. Geology 38, 491-494.

1123 Rodríguez-López, J.P., Melendez, N., De Boer, P.L., Soria, A.R., 2012. Controls on marine–erg
1124 margin cycle variability: aeolian–marine interaction in the mid-Cretaceous Iberian Desert System,
1125 Spain. Sedimentology 59, 466-501.

1126 Rodríguez-López, J.P., Clemmensen, L.B., Lancaster, N., Mountney, N.P., Veiga, G.D., 2014.
1127 Archean to Recent aeolian sand systems and their sedimentary record: current understanding and future
1128 prospects. Sedimentology 61, 1487-1534.

1129 Romain, H.G., Mountney, N.P., 2014. Reconstruction of three-dimensional eolian dune architecture
1130 from one-dimensional core data through adoption of analog data from outcrop. AAPG Bulletin 98, 1-22.

1131 Rubin, D.M., 1987. Cross-bedding, bedforms and paleocurrents. Geological Magazine 125, 469-
1132 470

1133 Rubin, D.M., 1990. Lateral migration of linear dunes in the Strzelecki Desert, Australia. Earth
1134 Surface Processes and Landforms 15, 1-14.

1135 Rubin, D.M., Hunter, R.E., 1983. Reconstructing bedform assemblages from compound
1136 crossbedding. In: M.E. Brookfield, T.S. Ahlbrandt (Eds.), Eolian Sediments and
1137 Processes, Elsevier, Amsterdam, pp. 407-427

1138 Rubin, D.M., Hunter, R.E., 1985. Why deposits of longitudinal dunes are rarely recognized in the
1139 geologic record. Sedimentology 32, 147-157.

1140 Rubin, D.M., Hunter, R.E., 1987. Bedform alignment in directionally varying flows. Science 237,
1141 276-278.

1142 Rubin, D.M., Tsoar, H., Blumberg, D.G., 2008. A second look at western Sinai seif dunes and their
1143 lateral migration. Geomorphology 93, 335-342.

1144 Santos, M.N.D., Chemale Jr, F., Dussin, I.A., Martins, M., Assis, T.A., Jelinek, A.R., Guadagnin,
1145 F., Armstrong, R., 2013. Sedimentological and paleoenvironmental constraints of the Statherian and
1146 Stenian Espinhaço rift system, Brazil. Sedimentary Geology 290, 47-59.

1147 Santos, M.N.D., Chemale Jr, F., Dussin, I.A., Martins, M.D.S., Queiroga, G., Pinto, R.T.R., Santos,
1148 A.N., Armstrong, R., 2015. Provenance and paleogeographic reconstruction of a mesoproterozoic
1149 intracratonic sag basin (Upper Espinhaço Basin, Brazil). Sedimentary Geology 318, 40-57.

1150 Sharp, R. P., 1963. Wind ripples. The Journal of Geology 71, 617-636.

1151 Scherer, C.M.S., 2000. Eolian dunes of the Botucatu Formation (Cretaceous) in southernmost
1152 Brazil: morphology and origin. Sedimentary Geology 137, 63-84.

1153 Scherer, C.M.S., 2002. Preservation of aeolian genetic units by lava flows in the Lower Cretaceous
1154 of the Paraná Basin, southern Brazil. Sedimentology 49, 97-116.

Scotti, A.A., Veiga, G.D., 2019. Sedimentary architecture of an ancient linear megadune (Barremian, Neuquén Basin): Insights into the long-term development and evolution of aeolian linear bedforms. Sedimentology 66, 2191-2213.

Shozaki, H., Hasegawa, H., 2022. Development of longitudinal dunes under Pangaean atmospheric circulation. Climate of the Past 18, 1529-1539.

Simplicio, F., Basilici, G., 2015. Unusual thick eolian sand sheet sedimentary succession: Paleoproterozoic Bandeirinha Formation, Minas Gerais. Brazilian Journal of Geology 45, 3-11.

Simpson, E.L., Eriksson, K.A., Eriksson, P.A., Bumby, A.J., 2002. Eolian dune degradation and generation of massive sandstone bodies in the Paleoproterozoic Makgabeng Formation, Waterberg Group, South Africa. Journal of Sedimentary Research 72, 40-45.

Stone, A.E.C., 2013. Age and dynamics of the Namib Sand Sea: A review of chronological evidence and possible landscape development models. Journal of African Earth Sciences 82, 70-87.

Tirsgaard, H., Øxnevad, I. E., 1998. Preservation of pre-vegetational mixed fluvio–aeolian deposits in a humid climatic setting: an example from the Middle Proterozoic Eriksfjord Formation, Southwest Greenland. Sedimentary Geology 120, 295-317.

Tseo, G., 1993. Two types of longitudinal dune fields and possible mechanisms for their development. Earth Surface Processes and Landforms 18, 627-643.

Tsoar, H., 1983. Dynamic processes acting on a longitudinal (seif) sand dune. Sedimentology 30, 567-578.

Tsoar, H., 1989. Linear dunes-forms and formation. Progress in Physical Geography 13, 507-528.

Tsoar, H., 2001. Types of aeolian sand dunes and their formation. In: N.J. Balmforth, A. Provenzale (Eds.), Geomorphological fluid mechanics. Springer-Heidelberg, Berlin, Germany, pp. 403-429.

Tsoar, H., Blumberg, D. G., Stoler, Y., 2004. Elongation and migration of sand dunes. Geomorphology 57, 293-302.

Uhlein, A., Chaves, M. L. D. S. C., 2001. O Supergrupo Espinhaço em Minas Geras e Bahia: correlações estratigráficas, conglomerados diamantíferos e evolução geodinâmica. Revista Brasileira de Geociências 31, 433-444 (In Portuguese with English abstract).

Wadhawan, S.K., 2020. Late Quaternary evolution of clustered parabolic megadunes in Thar Desert, India. In: Alsharhan, A.S., Glennie, K.W., Whittle, G.L. (Eds.), Quaternary Deserts and Climatic Change. CRC Press, London, pp. 185-195.

Wang, X., Dong, Z., Zhang, J., Qu, J., 2004. Formation of the complex linear dunes in the central Taklimakan Sand Sea, China. Earth Surface Processes and Landforms 29, 677-686.

Wilson, I. G., 1973. Ergs. Sedimentary geology 10, 77-106.

Yan, N., Colombera, L, Cosgrove, G.I.E., and Mountney, N.P., 2024. A 3D forward stratigraphic model of aeolian dune evolution for prediction of lithofacies heterogeneity. Computers and Geosciences 187, 105595. https://doi.org/10.1016/j.cageo.2024.105594.

Yu, X., Wang, C., Bertolini, G., Liu, C., Wang, J., 2021. Damp-to dry aeolian systems: Sedimentology, climate forcing, and aeolian accumulation in the Late Cretaceous Liyou Basin, South China. Sedimentary Geology 426, 106030. https://doi.org/10.1016/j.sedgeo.2021.106030

TABLE CAPTION

Table 1 - Summary of architectural elements described in the studied succession of the Galho do Miguel Formation and their interpretations.

FIGURE CAPTIONS

Figure 1 – Simplified geological map of the Southern Espinhaço Supergroup (SE Brazil) and location of the studied outcrops (Modified from CODEMIG, 2012a; CODEMIG, 2012b). Location of architectural panel and stratigraphic logs at Serra do Pasmar (B) and Morro Batatal (C) (Google Earth basemap, 2019). (D) Lithostratigraphy of the Southern Espinhaço Supergroup in studied area (modified from Martins-Neto, 2000; Chemale Jr et al., 2012).

Figure 2 – Synthetic scheme demonstrating the two models of linear dune development (simple and complex dunes) and its internal architecture (Modified from Scotti and Veiga, 2019). (A) Vertical accretion stage - concentric linear dune cross-section originated by a bimodal wind regime of airflows of similar sand-transport capacities. In this environment, the dune only moves longitudinally and aggrades upward. The bimodal foreset dip-azimuth is maintained, but the deposits have a low potential for accumulation and preservation. (B) Lateral migration stage – asymmetric linear dune profile produced by a bimodal wind regime of airflows with different sand-transport capacities. The main sand drift direction tends to be oblique to the crestline; this allows the lateral migration of dune coevally to the net longitudinal migration. The bimodal foreset dip-azimuth is missed, and the deposits have a higher potential for accumulation and preservation.

Figure 3 – Stratigraphic logs and distribution of the sedimentary facies throughout the studied succession, which compose four architectural elements. The location of each log is shown in Figure 1B, C. Almost 90% of succession is composed by the interbedding of compound sets of cross-strata, low-angle cross-stratification beds and planar-parallel sandstone strata. This arrangement indicates the deposition of complex linear megadunes, plinth areas, and inter-megadunes, respectively, in a dry environment (for further explanation see the text).

Figure 4 - Architectural panel 01 at the Serra do Pasmar locality (see Fig. 1B). (A) Photomosaic, (B) identifications by field drawings and photomosaic of the bounding surfaces and (C) architectural interpretation. The cross-section is perpendicular to the palaeotransport direction. Compound sets of trough cross-stratification are delimited by concave-up superimposition surfaces and interstratified with low-angle cross-bedded sets and planar-parallel sandstone strata elements. Simple sets of cross-strata overlap the succession. Low-angle cross-bedded sets are laterally connected and interdigitated to the lowermost part of foresets of the compound the cross-strata (white arrow), becoming progressively the planar-parallel sandstone strata element (dry inter-megadune deposits). The red arrow indicates an encroached contact between megadune and dry interdune deposits. (D) Rose diagram displaying the azimuthal distribution of foresets dipping of the compound cross-bedded sets. The black arrow displays the vector mean direction towards an azimuth of ca. 080°. “n” is the number of readings. (E) Poles of superimposition surfaces, demonstrating two main clusters of dip-direction of these surfaces. This preserved feature indicates two slipfaces opposite to each other, indicating the bimodal pattern of the palaeowind. “n” is the number of readings.

Figure 5 – Architectural panel 01 at the Morro Batatal locality (see Fig. 1B) in palaeotransport-transversal sections. (A) Photomosaic, (B) identifications by field drawings and photomosaic of the bounding surfaces, and (C) interpretation of the depositional architecture, showing the lateral and vertical geometric arrangement of the main architectural elements (a detailed description is in the text). The white arrow shows the abrupt contact between compound cross-bedded sets with low-angle cross-bedded sets and planar-parallel sandstone strata deposits, whereas the red arrow indicates a gradational contact between them. (D) Rose diagram showing the azimuthal distribution of foresets dipping of the compound cross-bedded sets. The black arrow displays the vector mean direction towards an azimuth of ca. 060°. “n” is the number of readings. (E) Rose diagram depicting the dip-azimuths of second-order bounding surfaces (superimposition surfaces). The black arrow demonstrates the mean vector (115° azimuth). “n” is the number of readings.

Figure 6 - Architectural panel 02 at Serra do Pasmar locality (see Fig. 1B) in palaeotransport-oblique sections.The three images represent: (A) the photomosaic, (B) identifications by field drawings and photomosaic of the bounding surfaces, and (C) the sketch of the interpretative architecture. The depositional architecture comprises the interlaying of compound sets of cross-strata, low-angle cross-stratatification bed and planar-parallel sandstone strata deposits. The foreset dip-azimuths and bounding surface dip-azimuth showed in the panel use a rose diagram oriented relative to the face of the observer; see the small circle at the bottom for azimuth value. The red arrow indicates an irregular or undulated first-order bounding surface (interdune surface) characterised by depressions and steps, limiting compound sets of cross-strata and low-angle cross-stratification bed in a sharp contact. The white arrow highlights the transitional contact between these architectural element types. Green arrows indicate the encroached contact between dune and interdune deposits. (D) Rose diagram displaying the azimuthal distribution of foresets dipping of the "compound cross-bedded sets". The black arrow displays the vector mean direction towards an azimuth of ca. 080°. “n” is the number of readings. (E) Rose diagram showing the dip-azimuths of second-order bounding surfaces (superimposition surfaces). The black arrow demonstrates the mean vector (146° azimuth). “n” is the number of readings.

Figure 7 – (A) Interdigitations between wedges of grainflow and subcritical climbing translatent strata at lowermost part of dunes cross-stratifications (palaeotransport-parallel cross-section). (B) Encroached relationship of planar-parallel sandstone strata at the toe-set of cross-stratifications. (C) The photography and (D) the architectural sketch demonstrate the downwind decrease of foreset dip-azimuths from high-angle (>15°) to low-angle cross-stratification and the relationship between dune cross-strata with interdune deposits (cross-section parallel to the sand palaeotransport).

Figure 8 - (A) The rose diagram displays the azimuthal distribution of foresets dipping of the "low-angle cross-stratifications bed" element. The black arrow displays the vector mean direction towards an azimuth

of ca. 120°. “n” is the number of readings. (B) The vortex ripples of the slightly asymmetric profile, straight sinuous crestlines, and peaked or rounded crests with some bifurcations. (C) Photography and (D) sketch of small erosive surface (white dotted line), which show geometry of small steps and depressions at palaeowind-parallel section. This surface is interpreted as first-order surface of type A (Basilici et al., 2021). The white arrows indicate this surface, which is related to ongoing dune migration over cohesive sand surfaces.

Figure 9 – (A) Simple sets of cross-strata arranged in tabular-shaped sets of cross-stratifications. The bottom and top of this architectural element are underlined by flat, irregular, and near-horizontal bounding surfaces (interdune surfaces - I). Erosive concave upward surfaces (R) are interpreted as reactivation surfaces. (B) Interdigitation of wedges of grainflow and subcritical climbing translatent strata at the lowermost part of tangential cross-stratifications. (C) Rose diagram of foresets dip azimuths of the simple sets of cross-strata element. The black arrow displays the vector mean direction towards an azimuth of ca. 075°. “n” is the number of readings.

Figure 10 – (A) Photomosaic and (B) the line drawing and architectural interpretation demonstrating a lens-shaped bed of planar-parallel sandstone strata interbedded with compound cross-bedded and low-angle cross-bedded sets element. The contact between these architectural elements may occur in a gradational or abrupt manner (see the text for a detailed description). (C) Horizontal to sub-horizontal laminations (< 5° inclined) of planar-parallel sandstone strata composed of inversely graded translatent strata. (D) Thin strata of cross-laminations interbedded with horizontal to sub-horizontal sandstone laminations. These deposits are interpreted as the product of sand deposition by vortex ripples and wind ripples, respectively.

Figure 11– Depositional model for the construction and accumulation of linear megadunes during the (A) concentric and (B) asymmetric stages in a Precambrian erg. This model is based on the lateral and vertical

distribution of the architectural elements of the studied succession. The accumulation of megadune and dry interdune strata occurred by climbing, aided further by the progressive rise of the accumulation surface. The progressive rise of accumulation surface was due to the increased sedimentary budget of the Proterozoic aeolian system, coupled with the gradual elevation of the water-table level, thereby enhancing the potential for accumulation within these ancient systems. The accumulation of dry interdune strata also seems to be controlled by the megadune morphology and migration patterns. Legend: AS – accumulation surface; WT – water table level.

Figure 12 – (A) Palaeodepositional model for the complex linear megadune system of the Galho do Miguel Formation. The large green arrow indicates the primary trend of the lateral migration of this megadune system. (B) Mega-bedform reconstruction based on the assemblages of the compound cross-strata. The red arrows represent the main airflows, and the blue arrow indicates the direction of megadune elongation. This arrangement is based on the studied deposits of the Galho do MIguel Formation coupled with the studies of Rubin and Hunter (1983) and Rubin and Carter (2006).

Figure 1

Click here to access/download;Figure;Figura 1.jpg

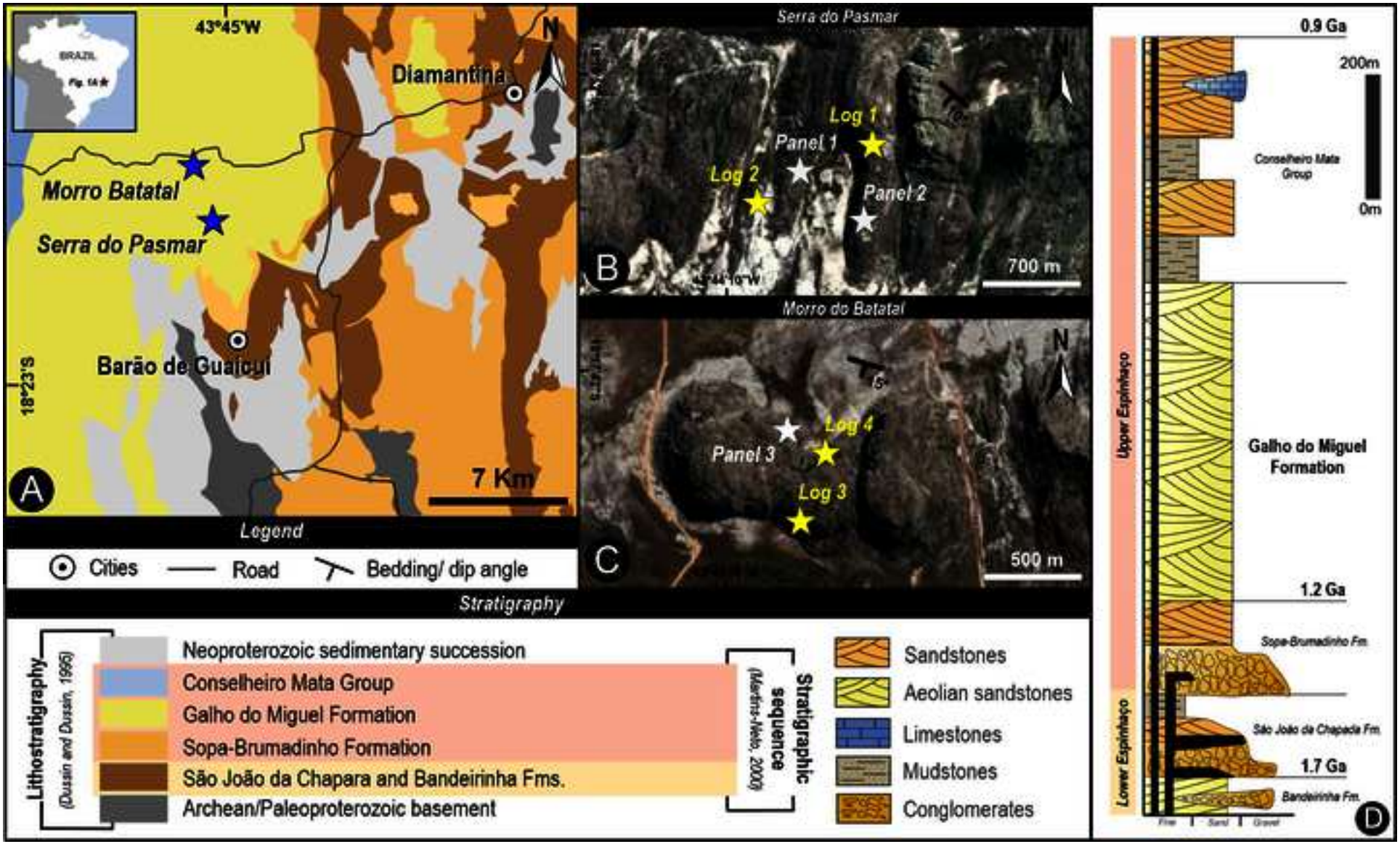

Figure 2

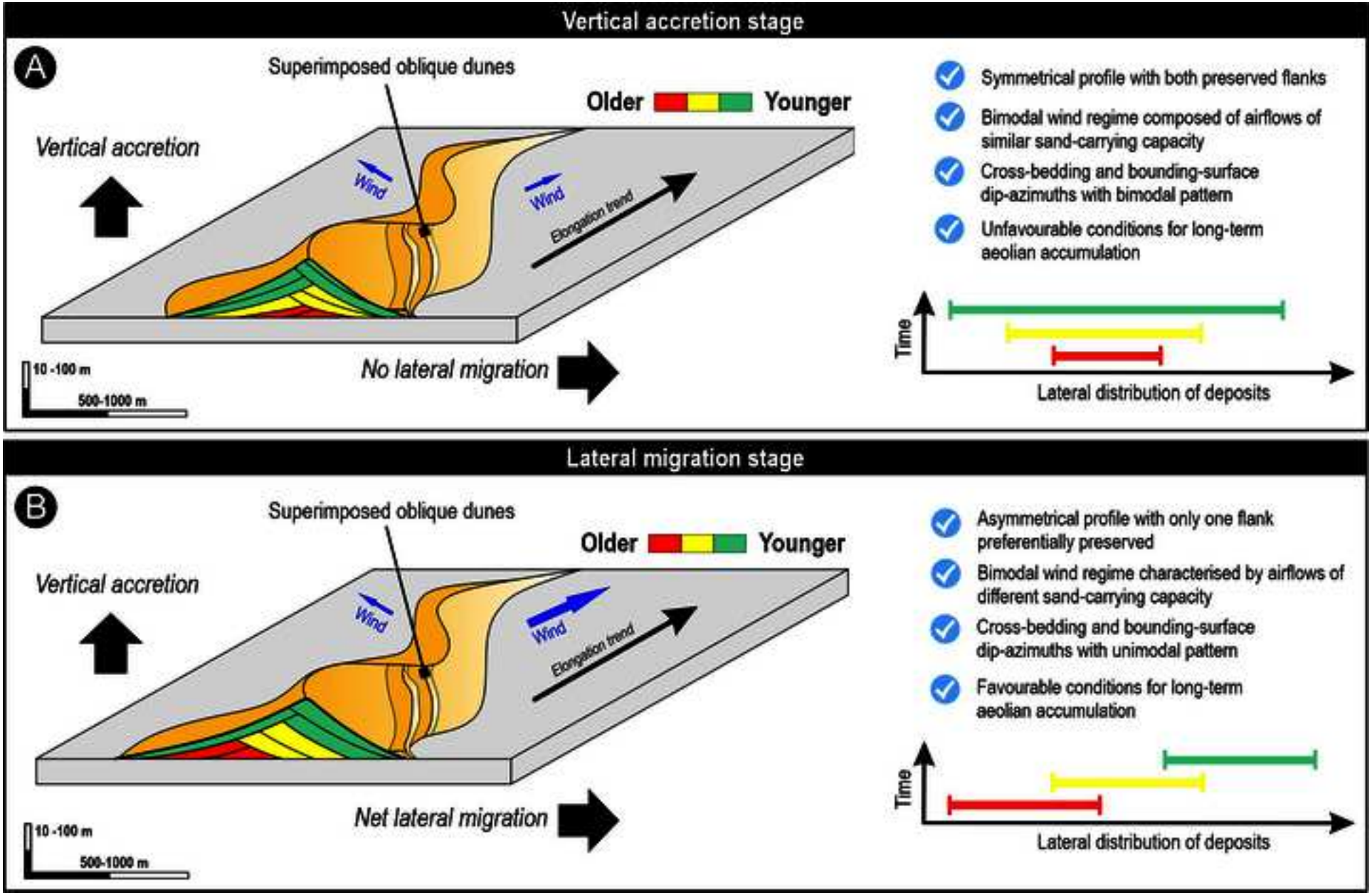

Figure 3

Click here to access/download;Figure;Figura 3.jpg

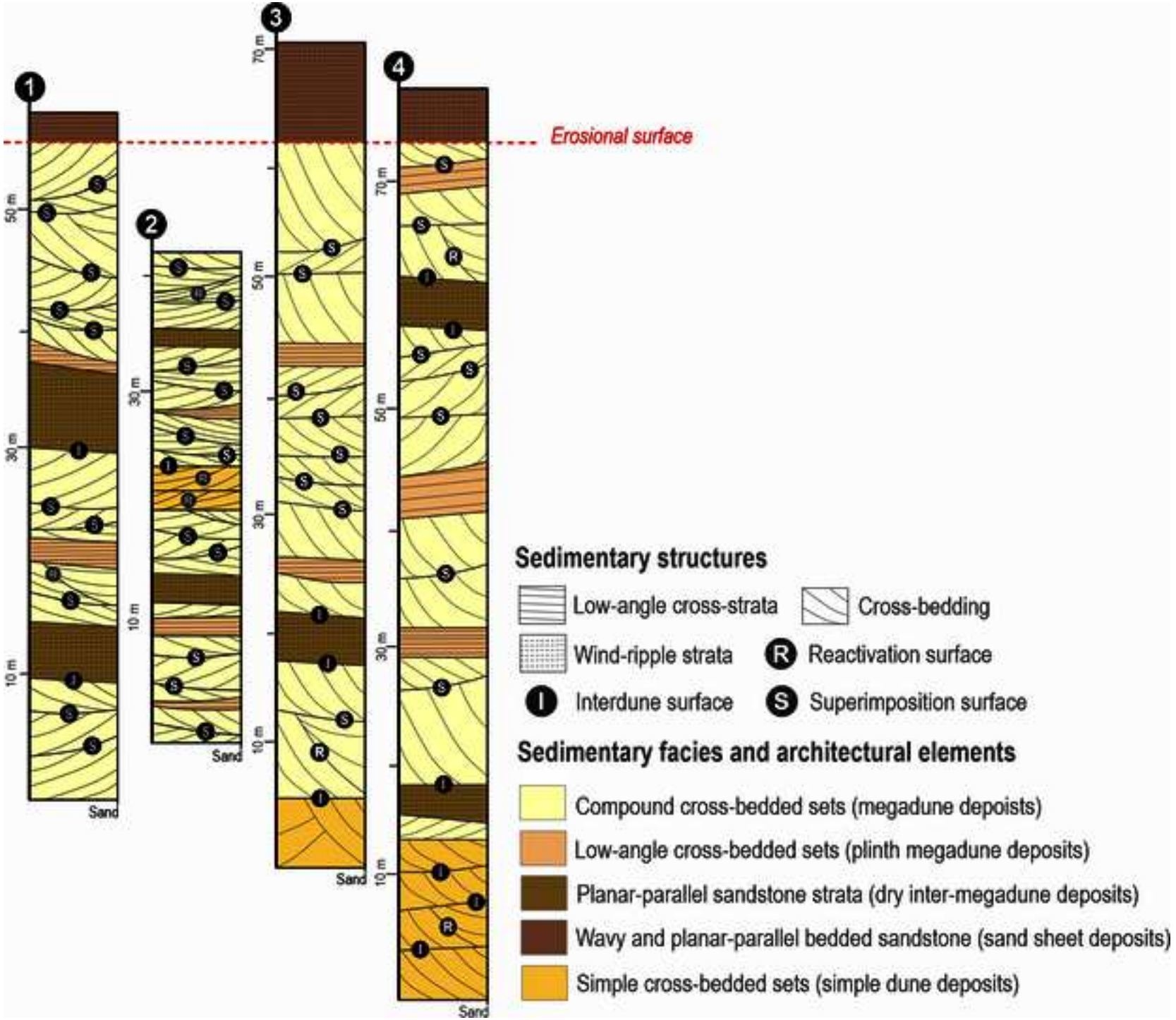

Figure 4

Click here to access/download;Figure;Figura 4.jpg

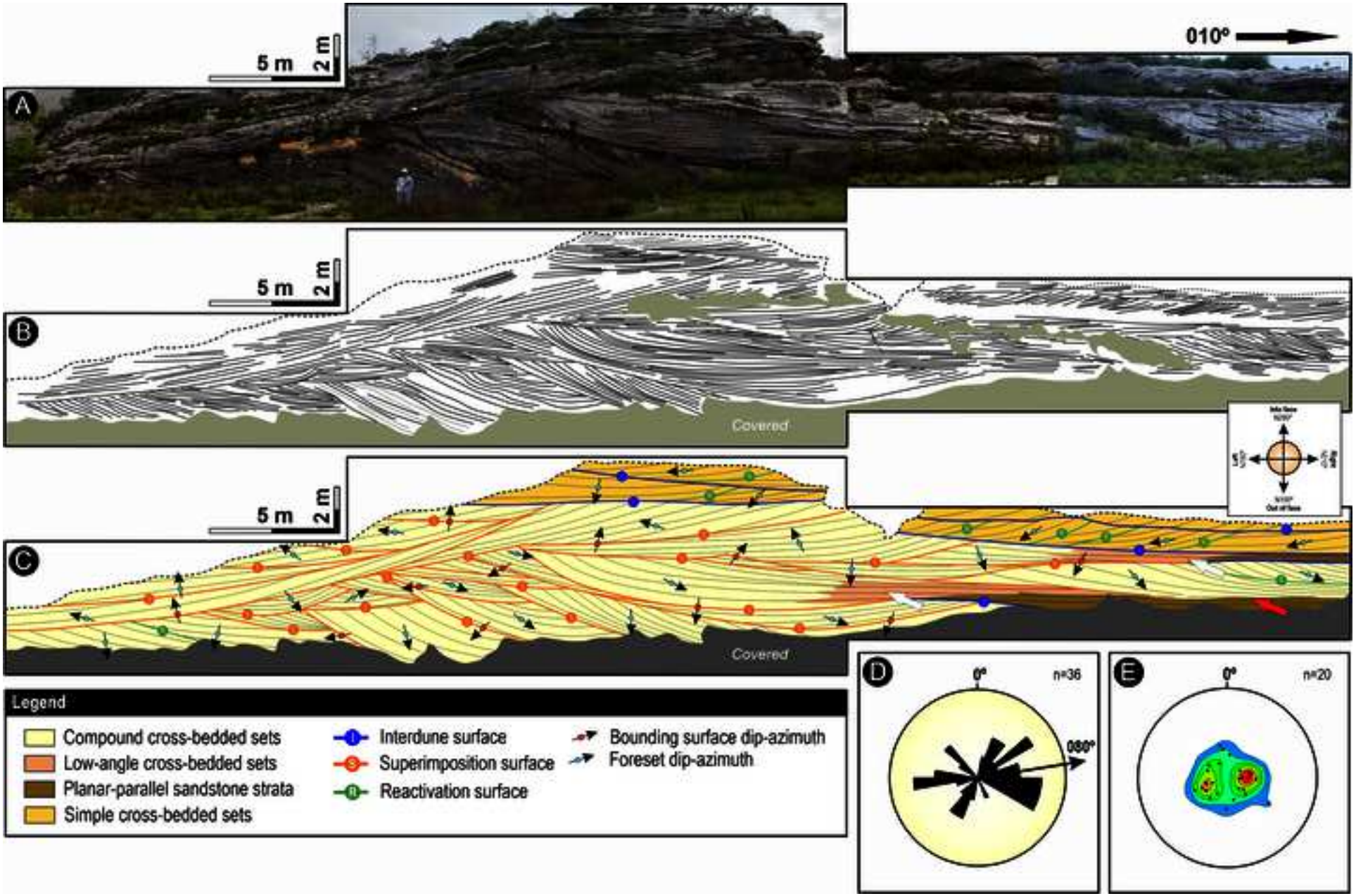

Figure 5

Click here to access/download;Figure;Figura 5.jpg

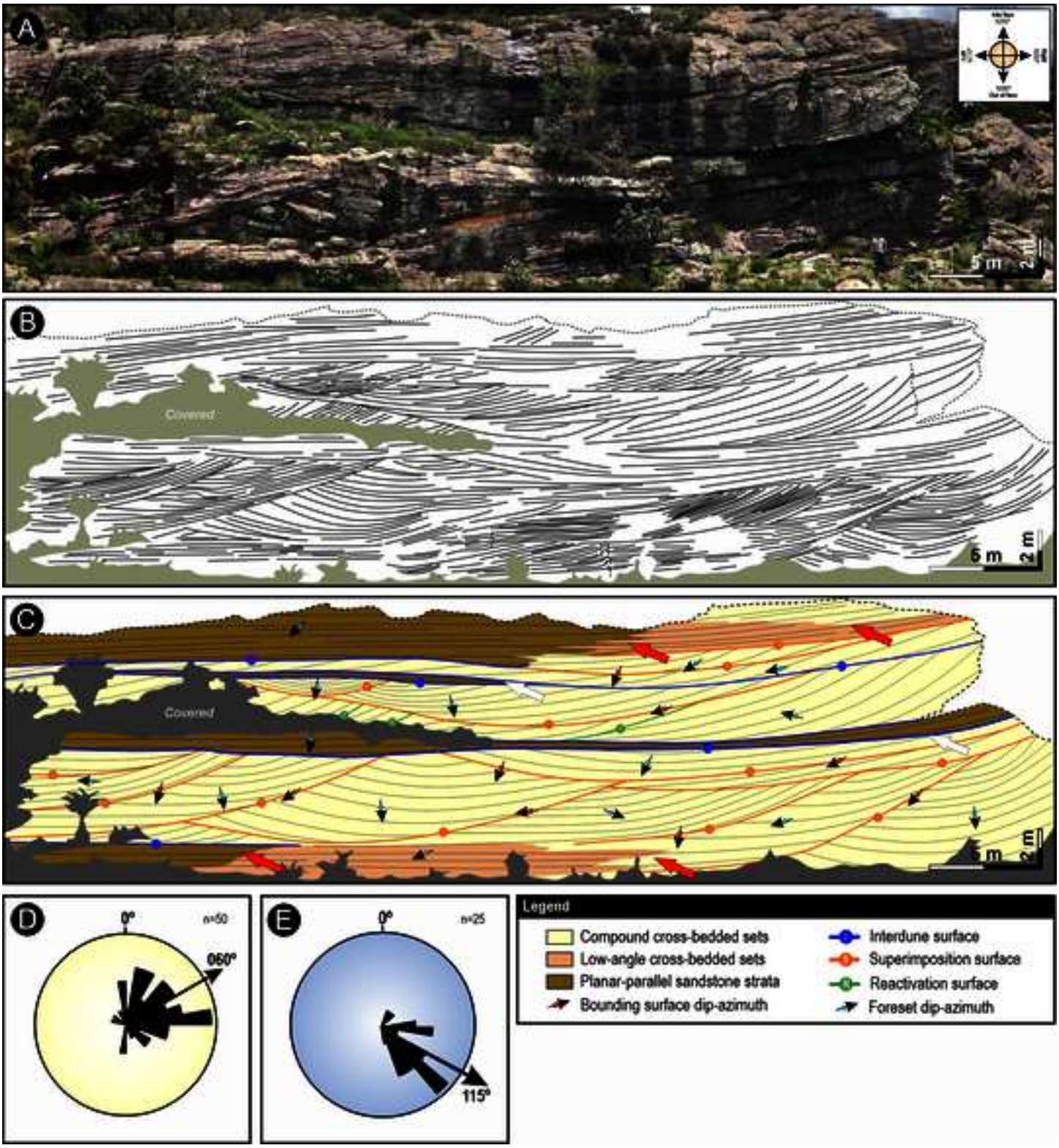

Figure 6

Click here to access/download;Figure;Figura 6.jpg

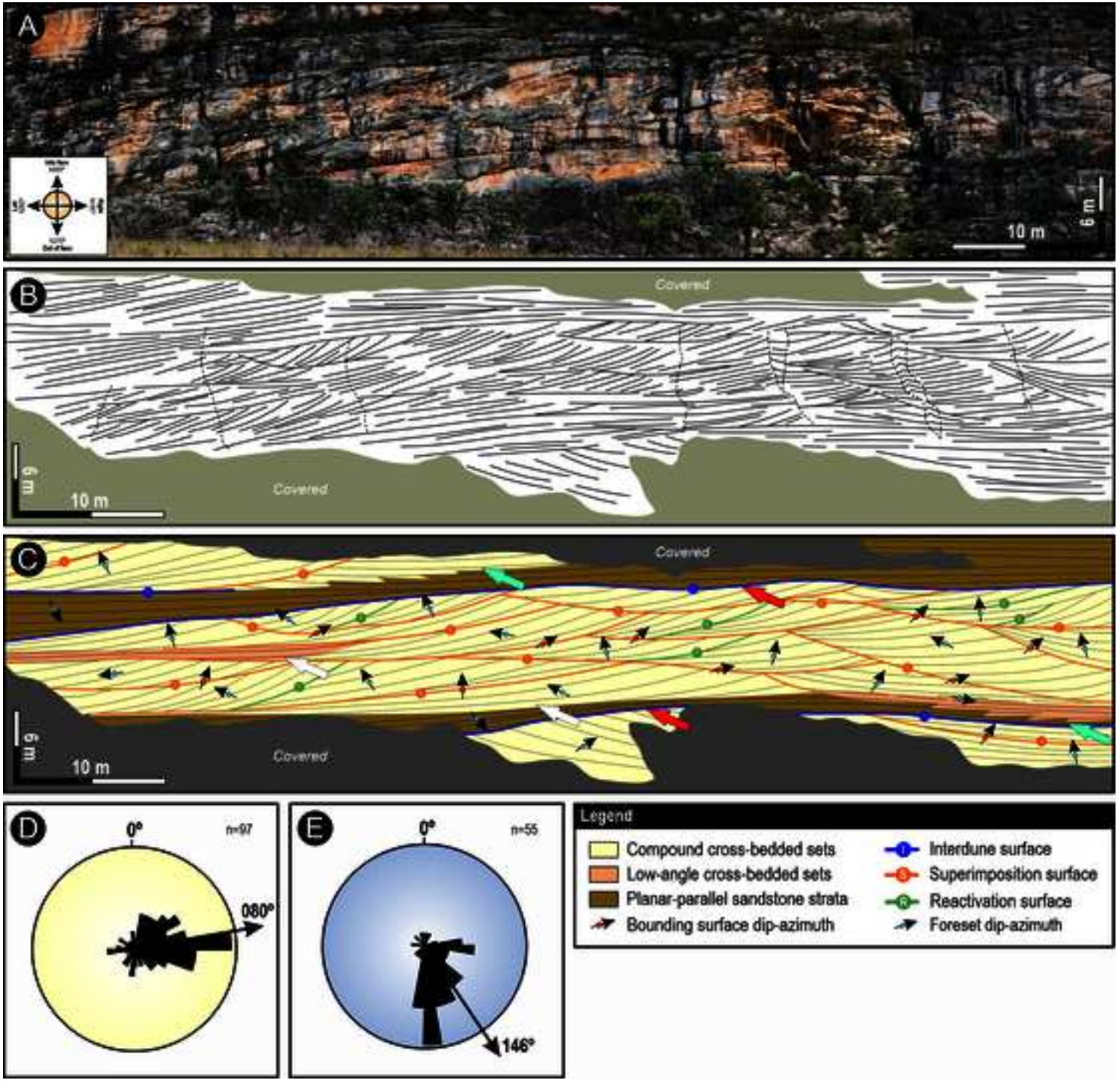

Figure 7

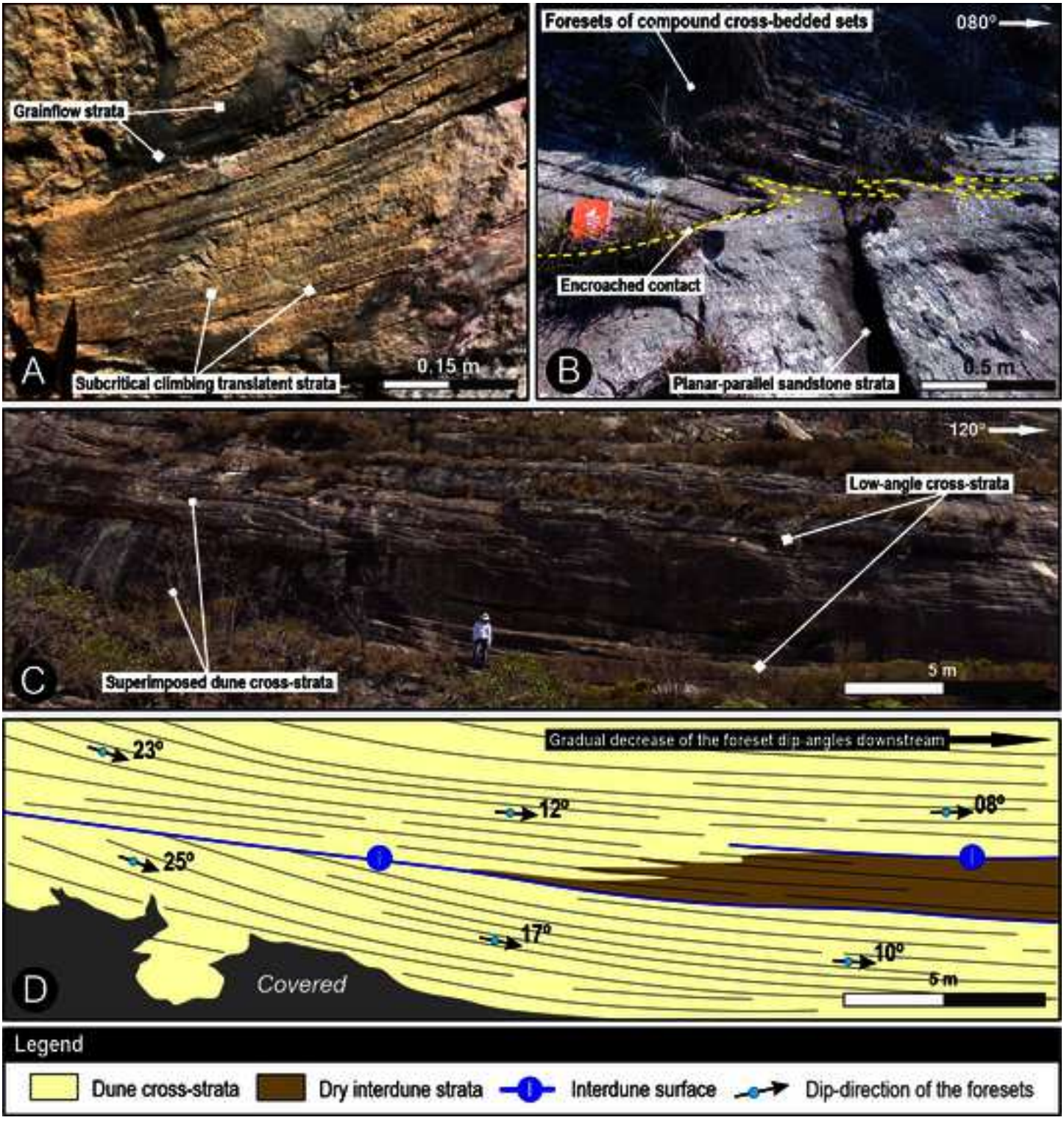

Figure 8

Click here to access/download;Figure;Figura 8.jpg

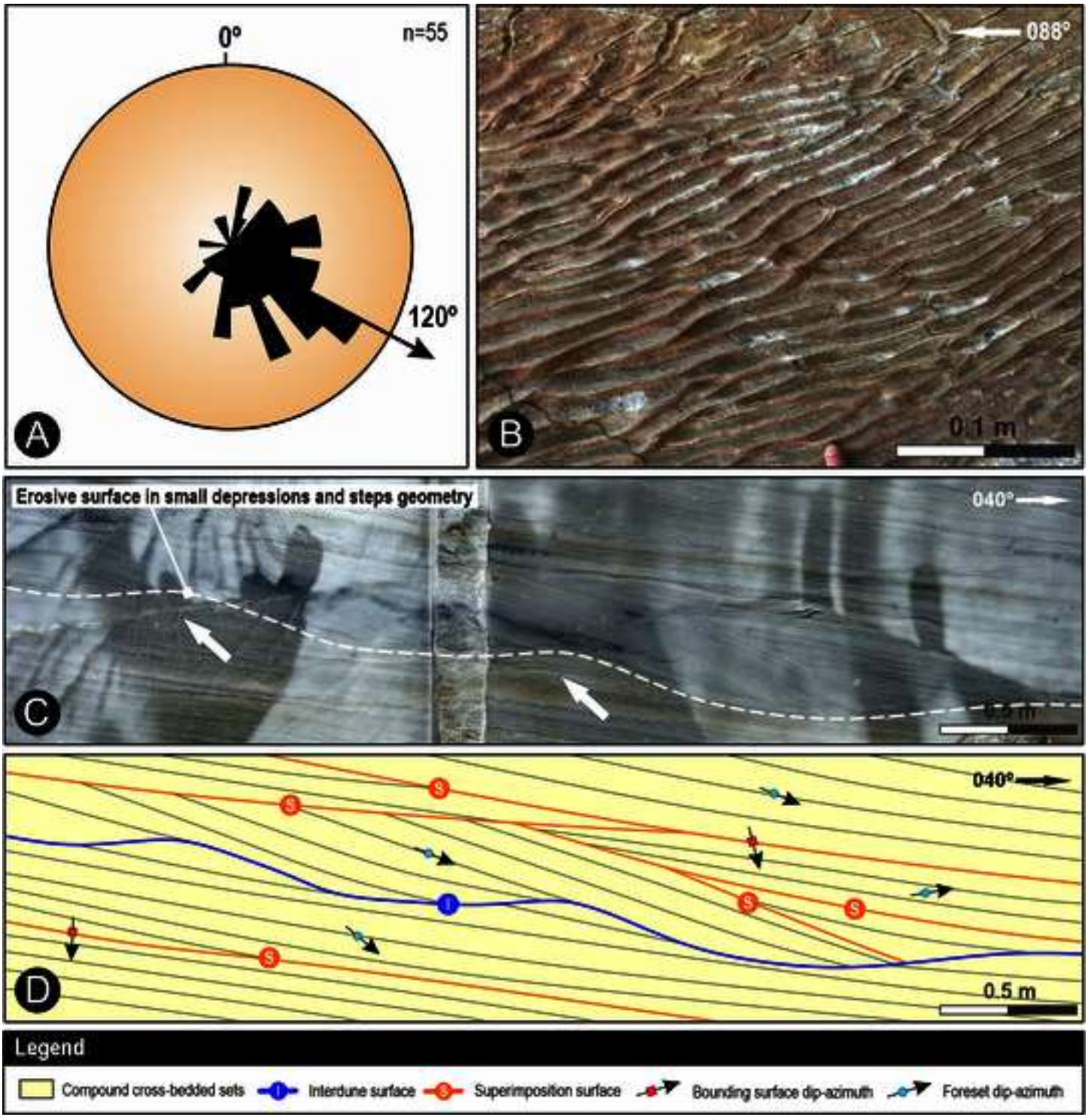

Figure 9

Click here to access/download;Figure;Figura 9.jpg

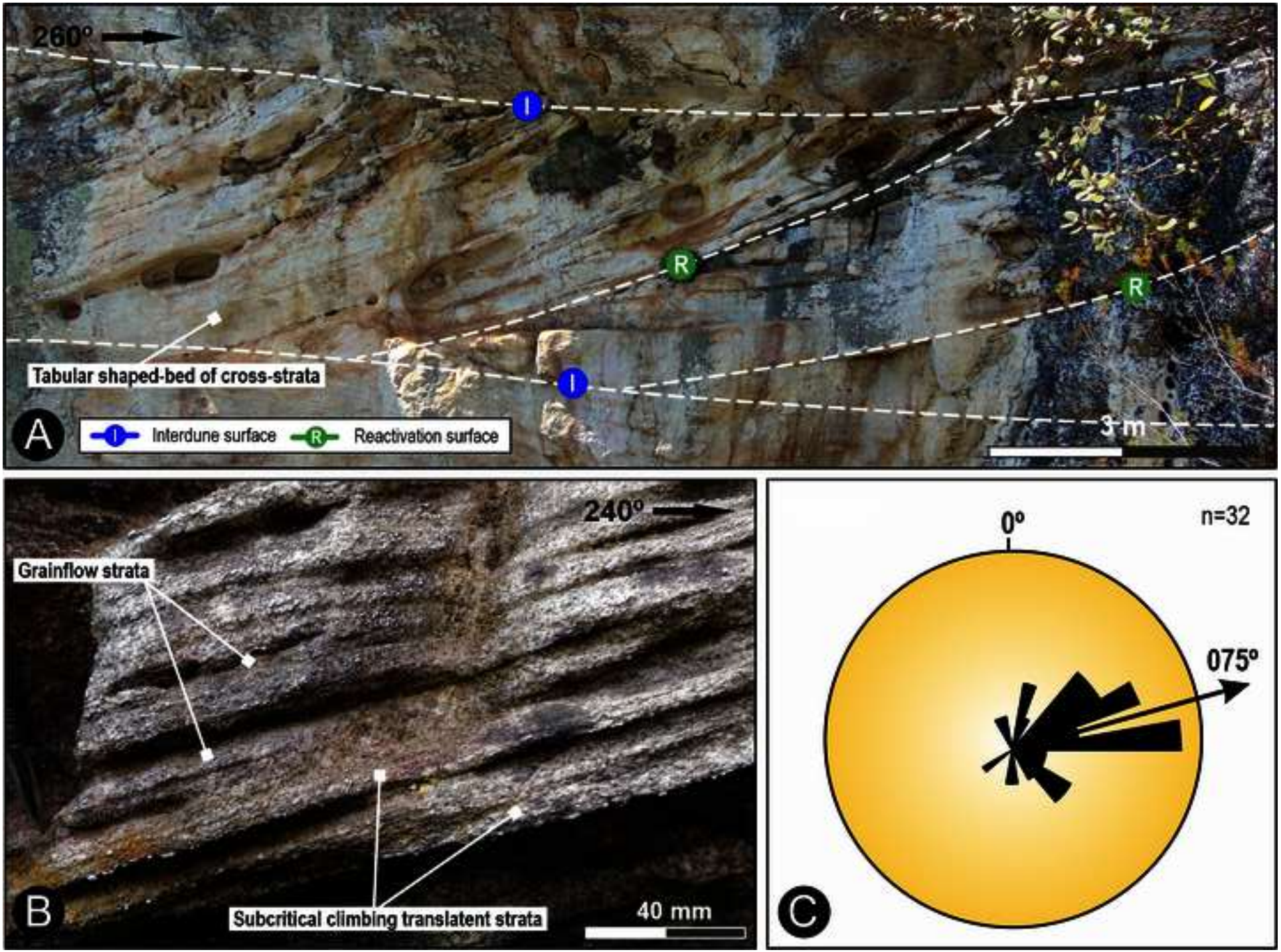

Figure 10

Click here to access/download;Figure;Figura 10.jpg

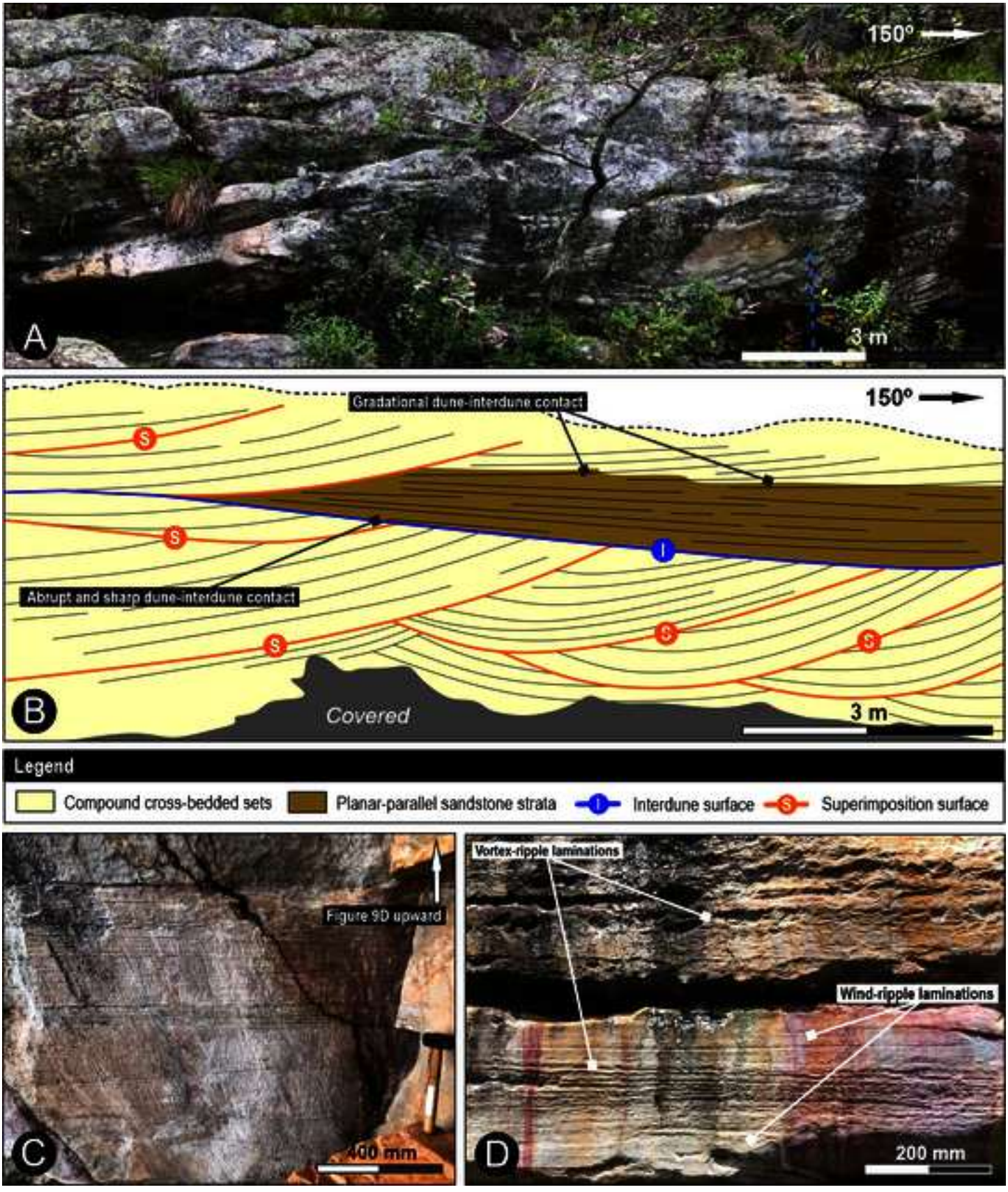

Figure 11

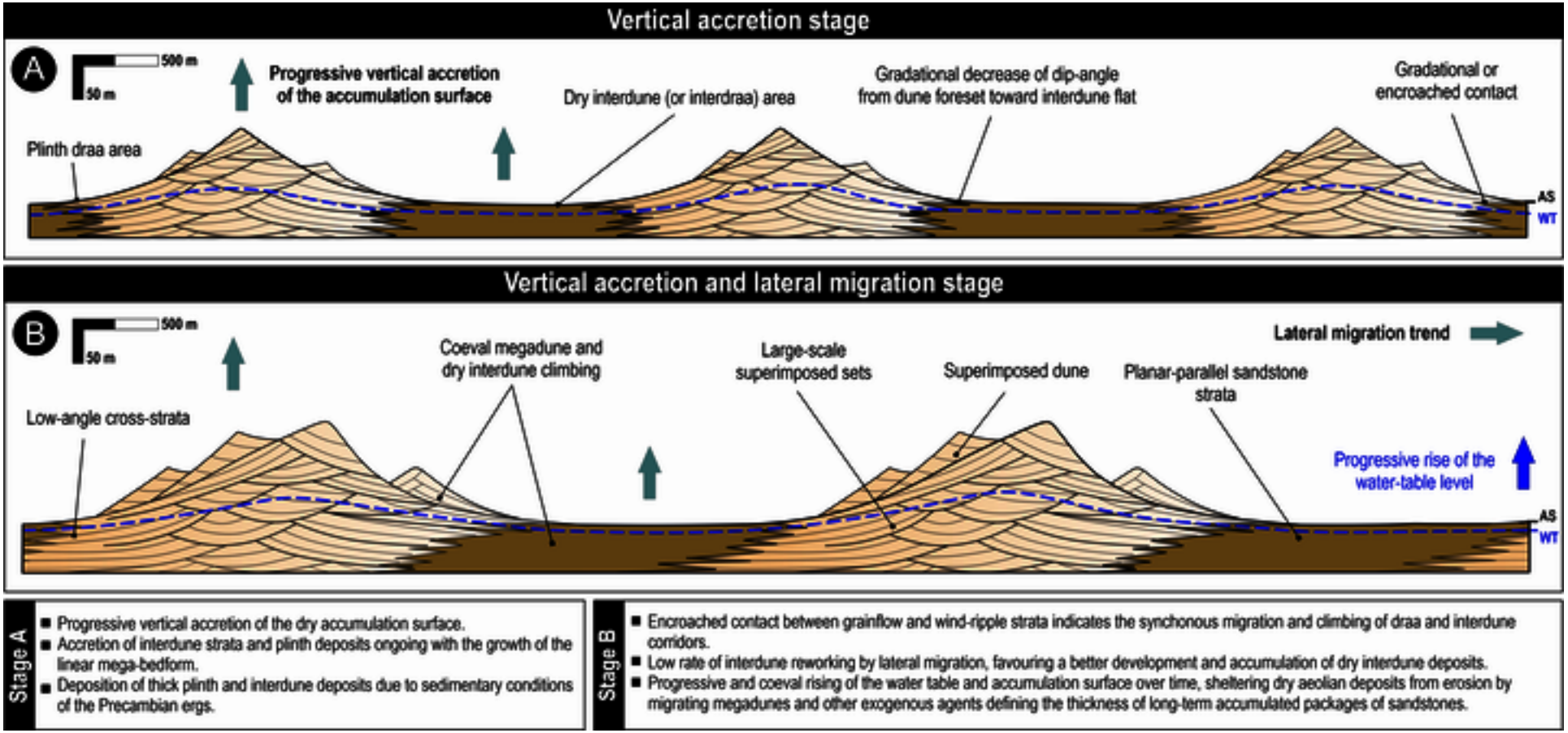

Figure 12

Click here to access/download;Figure;Figura 12.jpg

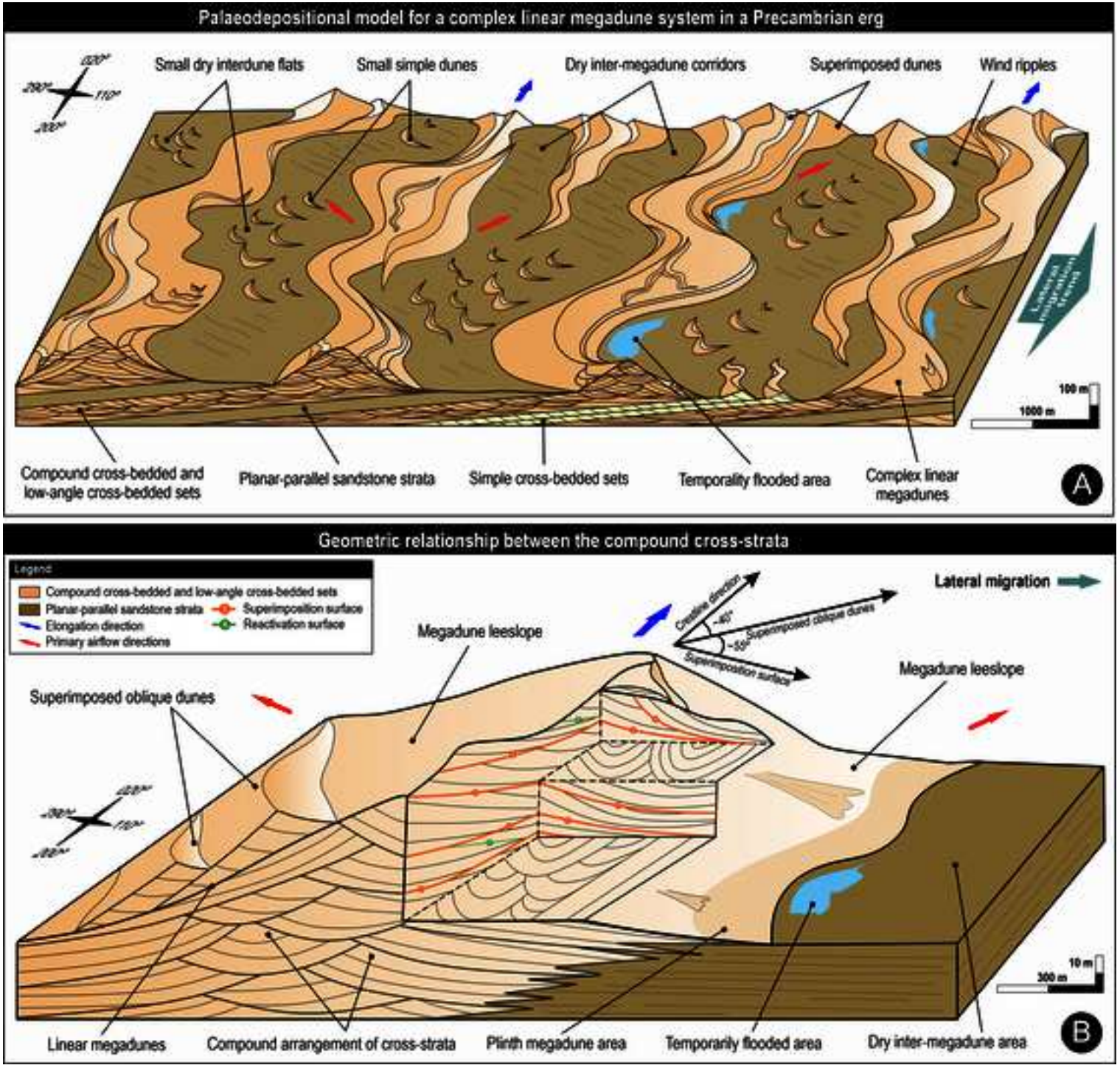

Architectural element	Depositional characteristics	Interpretation	References
Compound cross-bedded and low-angle cross-bedded sets	Interlayering of two main lithofacies: (i) "compound sets of cross-strata"; and (ii) "low-angle cross-stratification sets". The "compound sets of cross-strata" show a unimodal pattern of azimuths of foresets and superimposition surfaces towards 80º and 140°, respectively. "Low-angle cross-stratification sets" with low spread and average value towards ca. 120º azimuth. Dry interdune deposits are common and show contacts with superimposed cross-sets that record the encroachment of the latter over the former. The depositional architecture shows a complex architectural organisation composed by superimposed sets of variable thickness and geometry.	Complex linear megadune deposits: originated by migration of superimposed dunes and plinth dune areas. The superimposition occurred via climbing of dunes of different sizes and morphologies.	Brookfield (1977); Rubin and Hunter (1983); Kocurek (1991); Mountney and Howell, (2000); Mountney (2006a); Mountney and Thompson (2002); Abrantes Jr et al (2020).
Simple cross-bedded sets	Simple sets of tangential cross-stratifications with tabular-shaped geometry, up to 2 m thick and 4 to 40 m wide, limited at their top and bottom by interdune surfaces. Foreset dip-azimuths show a unimodal pattern and low-spread distribution with mean values of the azimuths towards 080°. The thickness and predominance of grain-flow strata in the lowermost parts of dune cross-stratification records simple dunes characterised by (i) well-developed slipfaces, (ii) high rates of dune migration and (iii) dune heights of more than 15 m.	Simple dune deposits; probably simple transversal dunes.	Brookfield (1977); Hunter (1977); Kocurek and Dott (1981); Kocurek (1991); Lancaster (1995); Mountney (2006a,b).
Planar-parallel sandstone strata	Lens-shaped beds (0.5 to 3 m thick) of laminated sandstones composed of horizontal to sub-horizontal laminations (inclined < 5°). Laminae are 5 to 10 mm thick. The individual lamination shows inverse grain grading. These deposits are usually interstratified with the compound cross-bedded and low-angle cross-bedded sets element and the stratigraphic relationship between them can occur in (i) gradational, (ii) encroached, or (iii) abrupt fashions. Locally thin beds of vortex-ripples laminations are present, indicating temporary developments of small and shallow ponds.	Dry inter-megadune deposits	Clemmensen (1989); Dong et al. (2004); Abrantes Jr. (2020); Wadhawan (2020).

TABLE 1

Declaration of interests

☒The authors declare that they have no known competing financial interests or personal relationships that could have appeared to influence the work reported in this paper.

☐The authors declare the following financial interests/personal relationships which may be considered as potential competing interests:

Áquila Ferreira Mesquita: Conceptualization, Investigation, Writing – Original Draft; **Giorgio Basilici**: Conceptualization, Investigation, Writing – Original Draft, Funding acquisition; **Alexandre Ribeiro Cardoso**: Conceptualization, Writing - Review & Editing; **Carlos Roberto de Souza Filho:** Funding acquisition, Investigation, Writing - Review & Editing; **Nigel P. Mountney**: Conceptualization, Writing - Review & Editing; **Luca Colombera**: Conceptualization, Writing - Review & Editing; **Grace I.E. Cosgrove**: Conceptualization, Writing - Review & Editing; **Juraj Janočko**: Conceptualization, Writing - Review & Editing; **Davi Machado Querubim**: Conceptualization, Investigation.

Declaration of interests

☒The authors declare that they have no known competing financial interests or personal relationships that could have appeared to influence the work reported in this paper.

☐The authors declare the following financial interests/personal relationships which may be considered as potential competing interests: